For Reference

NOT TO BE TAKEN FROM THIS ROOM

For Reference

NOT TO BE TAKEN FROM THIS ROOM

Ex libris
universitatis
albertaensis

The University of Alberta
Printing Department
Edmonton, Alberta

THE UNIVERSITY OF ALBERTA

MICROWAVE DRYING OF SOLIDS

by

©

GERALD BROCK ALLAN

A THESIS

SUBMITTED TO THE FACULTY OF GRADUATE STUDIES

IN PARTIAL FULFILMENT OF THE REQUIREMENTS FOR THE DEGREE

OF MASTER OF SCIENCE

DEPARTMENT OF ELECTRICAL ENGINEERING

EDMONTON, ALBERTA

June, 1967

UNIVERSITY OF ALBERTA

FACULTY OF GRADUATE STUDIES

The undersigned certify that they have read, and recommend to the Faculty of Graduate Studies for acceptance, a thesis entitled "Microwave Drying of Solids" submitted by Gerald Brock Allan in partial fulfilment of the requirements for the degree of Master of Science.

ABSTRACT

The application of high power microwaves to the removal of moisture from solids, though far from a new concept, has until recently been impractical due to lack of suitable microwave generation equipment. From the number of power microwave systems now in operation, it is apparent that this is no longer a serious problem.

Following a brief introduction to the drying of solids, an examination of the effects of microwave fields on wet materials is presented. Some basic relationships between power density, frequency, dielectric loss factor and penetration depth are established, and typical driers discussed.

Relatively basic empirical heat and mass transfer relations are inspected to check compatibility with microwave drier conditions. Terms to account for the effect of microwave fields are then introduced and prediction of the potential areas of advantage and disadvantage of microwave power are based on these expressions. The importance of the large positive internal temperature and vapour pressure gradients associated with microwave fields is apparent. Several factors involved in the design of a microwave drying system are subsequently discussed.

Some results of the microwave tray drying of a coarse sand and an inorganic hydrate in a 1 kw experimental system are presented. The drying curves are examined in detail and attempts made to provide qualitative explanations for all of the important features. Quantitative checks of several of the previously derived expressions are also made.

The economics of microwave drying are outlined, then illustrated by an example comparing air and microwave tray driers in a typical heat-sensitive powder drying application.

It is concluded that, in spite of many problem areas, sufficient advantages exist to justify the use of microwave power in drying.

TABLE OF CONTENTS

Page

LIST OF ILLUSTRATIONS iii

LIST OF TABLES iv

LIST OF SYMBOLS v

ACKNOWLEDGEMENT viii

1. INTRODUCTION .... 1.

  1.1 A Basis for Drying with Microwave Power .... 1.

  1.2 Scope of the Study .... 1.

  1.3 Terminology and Symbols .... 2.

2. A SUMMARY OF DRYING PRINCIPLES .... 4.

  2.1 Phases of Drying .... 4.

  2.2 Drying and Mechanisms of Moisture Movement .... 4.

3. ANALYSIS OF A MICROWAVE DRYING SYSTEM .... 8.

  3.1 Microwave Aspects of Drying .... 8.

  3.2 Constant Rate Drying .... 18.

  3.3 Diffusion-Controlled Drying of Non-Porous and Hygroscopic Materials .... 27.

  3.4 Capillary-Flow Drying of Porous Materials .... 32.

  3.5 Practical System Evaluation .... 39.

4. DRYING BEHAVIOR IN AN EXPERIMENTAL SYSTEM .... 45.

  4.1 Description of the Drier .... 45.

  4.2 Drying of a Granular Non-Hygroscopic Material .... 50.

  4.3 Dehydration of a Hydrated Inorganic Salt .... 59.

  4.4 Discussion of Rate Anomalies .... 65.

Page

5. AN ECONOMIC EVALUATION OF MICROWAVE DRYING .... 71.

5.1 Capital Costs .... 71.

5.2 Operating Costs .... 73.

5.3 Comparison with a Conventional Drier .... 75.

5.4 The Potential of Microwave Drying .... 81.

6. CONCLUSION .... 84.

REFERENCES .... 85.

LIST OF ILLUSTRATIONS

Figure Page

2.2.1 A Typical Water Sorption Isotherm Showing Drying Periods .... 6.

3.1.1 Complex Permittivity of Water as a Function of Temperature and Frequency .... 13.

3.1.2 Variation in Field Penetration Depth d_e for Water ..... 13.

3.1.3 Typical Microwave Drier Configurations .... 17.

3.2.1 Constant Rate Drying Model .... 23.

3.2.2 The Moisture Content Dependence of Power Density ...... 23.

3.2.3 Determination of Surface Temperature and Humidity ..... 23.

3.3.1 Typical Temperature Profiles for Diffusion-Controlled Tray Drying .... 31.

4.1.1 The Experimental Drying System .... 46.

4.1.2 Variation of Power Absorbed by a Water Load .... 49.

4.1.3 Division of Power between Two Water Loads .... 49.

4.2.1 Drying of a Coarse Natural Sand in a Microwave Tray Drier .... 51.

4.3.1 Dehydration of $CuSO_4 \cdot 5H_2O$ in a Microwave Tray Drier .... 60.

4.4.1 Lumped-parameter Equivalent Circuit of a Loop-coupled Multi-mode Cavity .... 67.

4.4.2 Calculated Dielectric Constant Variation of a Wet Sand with Moisture Content .... 67.

4.4.3 Resonant Frequency Spectrum of the Unloaded Cavity Near 2.46 GHz .... 69.

4.4.4 Resonant Modes in the Loaded Cavity for Drying of a 1.5 cm. Deep Sand Bed .... 69.

LIST OF TABLES

Table | Page

1. Drier Evaluation: Typical Product Specifications and Drier Schematic Diagrams .... 77.

2. Drier Evaluation: Specifications for Air and Microwave Tray Driers Suitable for Moderately Heat-Sensitive Powders .... 78.

3. Drier Evaluation: Capital and Operating Costs .... 79.

LIST OF SYMBOLS

1. Microwave Engineering

d_e = field penetration depth, m.
$\bar{D}$ = electric (vector) field displacement (or flux dens.), coul./m^2.
e = 2.718..., the base of natural logarithms
$\bar{E}$ = electric (vector) field intensity, volts/m.
E_o = electric field intensity in free space (or air), volts/m.
E_t = transmitted electric field intensity (complex), volts/m.
f = frequency, Hz.
$\underline{f}_c$ = waveguide cutoff frequency, Hz.
$\bar{H}$ = magnetic (vector) field intensity, amps./m.
$\underline{j}$ = $\sqrt{-1}$, associated with the imaginary part of complex quantities.
$\bar{M}$ = magnetic (vector) displacement current, weber/m^2-sec.
$\bar{P}_d$ = time-average power dissipated in a dielectric, watts
t = temperature, °C
T = absolute temperature, °K
$\tilde{T}$ = wave transmission coefficient, dimensionless
dv = volume differential, m^3.
VSWR = voltage standing wave ratio, dimensionless
x, y = directions perpendicular to direction of wave propagation
$\underline{\bar{X}}$ = Π/Π_o; see page 24
z = direction of wave propagation
Z = complex wave impedance in a finite region, ohms

α_d = dielectric loss attenuation constant, m.$^{-1}$
β = dielectric phase constant, m.$^{-1}$
δ = dielectric loss angle (between ε', ε''), radians
ε = complex permittivity, farads/m.
ε' = dielectric constant (Re{ε}), f./m.
ε'' = dielectric loss factor (Imag{ε}), f./m.
ε_o = permittivity of free space = 8.854×10^{-12}f./m.
ε_{ds} = permittivity of the dry solid, f./m.
ε_w = complex permittivity of water, f./m.
ε_r' = relative dielectric constant = $\varepsilon'/\varepsilon_o$, dimensionless
ε_r'' = relative dielectric loss factor = $\varepsilon''/\varepsilon_o$, dimensionless
γ_2 = $\alpha + j\beta$ = complex propagation constant in the dielectric, m.$^{-1}$
η = intrinsic wave impedance, ohms
η_o = wave impedance of free space ≃ 377 ohms
κ = parameter group; see page 63
Π = dissipated power density, watts/m^3.
Π' = dissipated power density, BTU/hr.ft^3. = $0.0966\ \Pi$
θ = time, sec. (unless other units are noted)
σ = conductivity, mho
τ_d = di-polar molecule frequency response time constant, sec.
ω = angular frequency, rdns./sec.$^{-1}$
μ_o = permeability of free space = $4\pi \times 10^{-7}$ henry/m.
∇^2 = Laplacian operator

2. Chemical Engineering

A = evaporating surface area, ft^2.
A_u = ratio of tray outside unwetted surface to evaporating surface
c = specific heat of the wet material, BTU/lb.°F
c_s = specific heat of 1 lb. of dry air plus the moisture it contains (humid heat), BTU/lb.°F
d = bed depth, ft.
d' = mean depth of internal evaporating surfaces, ft.
$\tilde{D}$ = diffusivity of water vapour through air, ft^2/hr.
D_c = hydraulic radius (see page 27), ft.
D_p = average particle diameter, ft.
F_1 = bed porosity, dimensionless
F_2 = bed structural factor; see page 37
g = acceleration of gravity, ft./sec^2.
G = mass velocity of air, lb.mass/hr.ft^2.
G_v = mass velocity of water vapour, lb.mass/hr.ft^2.
G_w = diffusional mass flow rate of water, lb.mass/hr.ft^2.
h_c = convective heat transfer coefficient, BTU/ft^2 hr.°F
h_L = fluid head loss, ft. of water
h_r = radiative heat transfer coefficient, BTU/hr.ft^2°F
h_t' = total heat transfer coefficient, BTU/hr.ft^2°F
H = absolute humidity, lb.water/lb.dry air
H_a = abs. humidity of air remote from an evaporating surface
H_m = logarithmic mean absolute humidity, lb./lb.dry
H_r = relative humidity, percent
H_s = absolute humidity of saturated air, lb./lb.dry
H_1 = inlet air absolute humidity, lb./lb.dry
H_{s2} = air saturation absolute humidity at drier exhaust, lb./lb.dry
ΔH^0 = heat of dehydration, BTU/lb.mole
k_T = thermal conductivity of wet material, BTU/ft.hr.°F
k_w = moisture conductivity (see page 33), ft^2/hr.
K_G = mass transfer coefficient, lb.mass/hr.ft^{2}atm.
K', K_G' = modified mass transfer coefficients (see pages 20, 21), lb.mass/hr.ft^{2}atm.
$\tilde{K}$ = hydrate equilibrium constant
m, n = empirical exponents; see page 19
M_a = molecular weight of air, lb./lb.mole
M_w = molecular weight of water, lb./lb.mole
N = normality (solute equivalents per litre of solution)
p_a = partial pressure of air remote from evaporating surface, atm.
p_{fm} = logarithmic mean partial pressure of air in the boundary film, atm.
p_{fs} = partial pressure of air at the evaporating surface, atm.
p_{ft} = partial pressure of air at the upper surface of the boundary film, atm.
p_M = maximum absolute vapour pressure, lb./in^{2}abs.
p_o = saturation vapour partial pressure at temp. T, atm.
p_T = total pressure, atm.
p_w = partial pressure of water vapour, atm.
p_{wa} = partial pressure of water vapour remote from evaporating surface, atm.
p_{ws} = partial pressure of water vapour at an evaporating surface, atm.
$\dot{q}_t$ = rate of total heat flow, BTU/sec.

r = effective particle radius, ft.
r_c = capillary radius, ft.
$\underset{\sim}{R}$ = universal gas constant, units as noted
$\bar{R}$ = $W/\{W + \rho_w/\rho_s\}$; see page 11
S = particle surface area, ft.^{2}
t_a = air temperature remote from evaporating surface, $^\circ$F
t_m = mean temperature of the bed, $^\circ$F
t_M = maximum temperature of the bed, $^\circ$F
t_s = evaporating surface temperature, $^\circ$F
t_{wa} = wet-bulb temperature of air remote from evaporating surface, $^\circ$F
t_2 = drier outlet air temperature, $^\circ$F
t_1 = drier inlet air temperature, $^\circ$F
v_M = vapour specific volume at p_M, ft.^{3}/lb.mass
v_w = water load volume, milliliters
v_s = vapour specific volume at p_{ws}, ft.^{3}/lb.mass
V = experimental drier hot air gun voltage, volts
V_f = water flow velocity, ft./sec.
w = absolute water content, lb.water
$\bar{w}_s$ = dry solid weight, lb.
$dw/d\theta$ = absolute drying rate, lb.water/hr.
W = relative moisture content, lb.water/lb.dry solid
$dW/d\theta$ = relative drying rate, lb.water/lb.dry solid-hr.
W_c = critical moisture content, lb./lb.dry
W_e = equilibrium moisture content, lb./lb.dry
W_o = initial moisture content, lb./lb.dry
$\bar{x}$ = moles of water released per mole of hydrate
x_o = bed length, ft.
X = packing factor, dimensionless
y = fraction of fine pores at the surface
Y = moisture permeability, lb./hr.ft.atm.
$\tilde{Z}$ = vapour compressibility factor, dimensionless

ℓ = capillary liquid height, ft.
Γ = capillary suction potential, ft. of water
Γ_1 = suction potential at the bed surface, ft. water
Γ_2 = suction potential at the bed mean water level, ft. water
θ = time, hr. (unless otherwise noted)
λ_s = latent heat of vapourization at an evaporating surface, BTU/lb.
μ = dynamic viscosity of the gas film, lb./hr.ft.
ρ = density of the wet material, lb.mass/ft.^{3}
ρ_f = density of air in the boundary film, lb.mass/ft.^{3}
ρ_s = absolute density of dry solid, lb.mass/ft.^{3}
ρ_w = density of water, lb.mass/ft.^{3}
σ_T = surface tension of water, lb./sec.^{2}

ACKNOWLEDGEMENT

The writer wishes to express sincere gratitude to his supervisor, Dr. W. A. G. Voss, for providing the opportunity to study a practical industrial microwave process and for the unfailing interest, encouragement and assistance without which the work could not have been completed.

Financial assistance provided by the National Research Council under Grant No. A2272, "Applications for High Power Microwave", is also gratefully acknowledged.

The power source and control system used in the experimental work were loaned to the University by Durand Machine Co. of New Westminster, B.C.

Special thanks are extended to Mr. W. Tinga and Mr. I. Grisch for their help in the experimental work.

1. INTRODUCTION

1.1 A Basis for Drying with Microwave Power

Although many different means exist for the removal of water from solid materials, drying remains a major problem in many industries. Where long drying times are required, large and costly equipment must be built and operated to handle any substantial amount of product. In order to dry heat-sensitive materials, either very slow drying is necessary or very expensive vacuum or freeze driers must be used. The drying stage usually contributes an appreciable portion of the overall processing cost in such applications.

The direct heating characteristic of microwave energy and the high dielectric loss of water at microwave frequencies should combine to produce drying rates far in excess of those now obtainable by most conventional drying methods. Because heat is not transferred primarily by mass movement or contact, lower material temperatures should also be possible if required. Microwave energy can be introduced into almost any drier configuration so that great flexibility of design is available for microwave driers. Finally, the cost of generating microwave energy has decreased to the point at which it now appears competitive in many cases with conventional energy costs. If a firm basis for these statements can be established, microwave power drying may justifiably be considered an industrially feasible process.

1.2 Scope of the Study

The following study is an attempt to examine microwave drying from analytical, experimental and economic viewpoints. It has been written

to provide, as nearly as possible, a balance between microwave and chemical engineering considerations so as to be of use to both disciplines. To avoid the common mistake of applying standard expressions to the explanation of phenomena which may violate conditions under which such expressions were derived, a fairly basic approach to each analysis has been taken. All necessary assumptions are reviewed for compatibility with microwave conditions. While this procedure leads in some cases to a rather lengthy evaluation, the amount of detail will serve both to strengthen any conclusions drawn and to establish a firm basis for design of actual drying systems.

The systems and materials chosen for evaluation are admittedly among the simplest possible and as such are not typical of most practical drying problems. Because of their relative simplicity, however, it was possible to provide a quite complete qualitative picture of the drying as well as to check several of the analytical expressions quantitatively. It is hoped that application to more complex systems can be approached with confidence as a result.

1.3 Terminology and Symbols

For this study, the mks rationalized system of electromagnetic units is used in conjunction with British standard engineering units. While some nuisance in converting between these may be encountered, the systems represent units in most common usage. Symbols may differ occasionally from those normally associated with certain quantities, but this has been done only as necessary to provide each quantity with a unique symbol. Otherwise, standard symbols of both microwave and chemical engineering practice have been employed.

Moisture content will be referred to the weight of dry material

(dry-basis moisture content) rather than to the weight of wet material (wet-basis moisture content). While wet-basis figures are common in wood products industry literature, the advantage of being a linear function of contained liquid weight has led to the more general acceptance of dry-basis moisture content. For this reason also, the choice of dry-basis is convenient when dealing with other systems of units and with electromagnetic relationships.

2. A SUMMARY OF DRYING PRINCIPLES

2.1 Phases of Drying

Water may be held by a material in a layer of free water on the material external surfaces, in pores within the material, or in the solid itself, as chemically bound water. Corresponding to the removal of water in each circumstance, a distinct drying behavior will be observed. Since least energy is required to evaporate surface water, it will be carried away first. The wet material will dry just as if it was a body of water. Drying during this phase is called 'constant-rate' drying for reasons which will become apparent later.

When surface water has been removed, water will be drawn next from within the pores of the material. More energy is required for evaporation in this case since the vapour pressure inside a pore is lower than that over a flat surface. The drying rate usually decreases with time as moisture movement encounters increasing internal flow resistance. Finally, the bed of material is left with water remaining only in the finest pores and capillaries, and in the solid itself. To remove the latter moisture, chemical bonds must be broken, either at the solid surfaces for adsorbed moisture, or deep within the solid as for a hydrated salt. Drying in this phase is characterized by rate falling with time, long duration, low thermal efficiency and high material temperatures. These final two phases of drying are known as 'falling rate' periods.

2.2 Drying and Mechanisms of Moisture Movement

For purposes of analysis, moisture movement can be attributed at various times to one or more of several distinct physical mechanisms.

Free water over an external surface will evaporate using heat from the surrounding air. Vapour diffuses from the air-water interface through a stagnant air boundary layer and into the flowing air beyond. Evaporation rate depends only on the heat and mass transfer nature of the system of surface passing air and is normally unaffected by wet material characteristics.

As external water is depleted, the evaporating surfaces will begin to recede into the interstices and openings of a porous material. Smaller pores will draw water from the larger pores by capillary action and, if enough of the surface is covered by small pores, will succeed in maintaining an almost completely wet external surface. Air will enter the substance intermittently through transient openings in the water layer. This meta-stable situation can extend constant rate drying well past the point of bed saturation moisture content. When resistance to capillary flow increases to the point at which the small capillaries can no longer deliver the flow of water required for full-surface constant rate drying, the surface layer becomes discontinuous.

It is at this stage that falling-rate period drying begins. So long as the small capillaries are able to draw water from within the bed, drying will proceed from water transported to the surface. Usually, only minor evaporation occurs inside the material. When the water reservoirs of the small capillaries fail, the external surface dries to its equilibrium moisture content and evaporation continues from pore menisci inside the bed. Drying rate will then be limited by vapour flow characteristics within the material.

Many substances will shrink as moisture is removed, giving the appearance of moisture movement outward. The effect of this on drying behavior will be similar to that observed for capillary-flow limited drying.

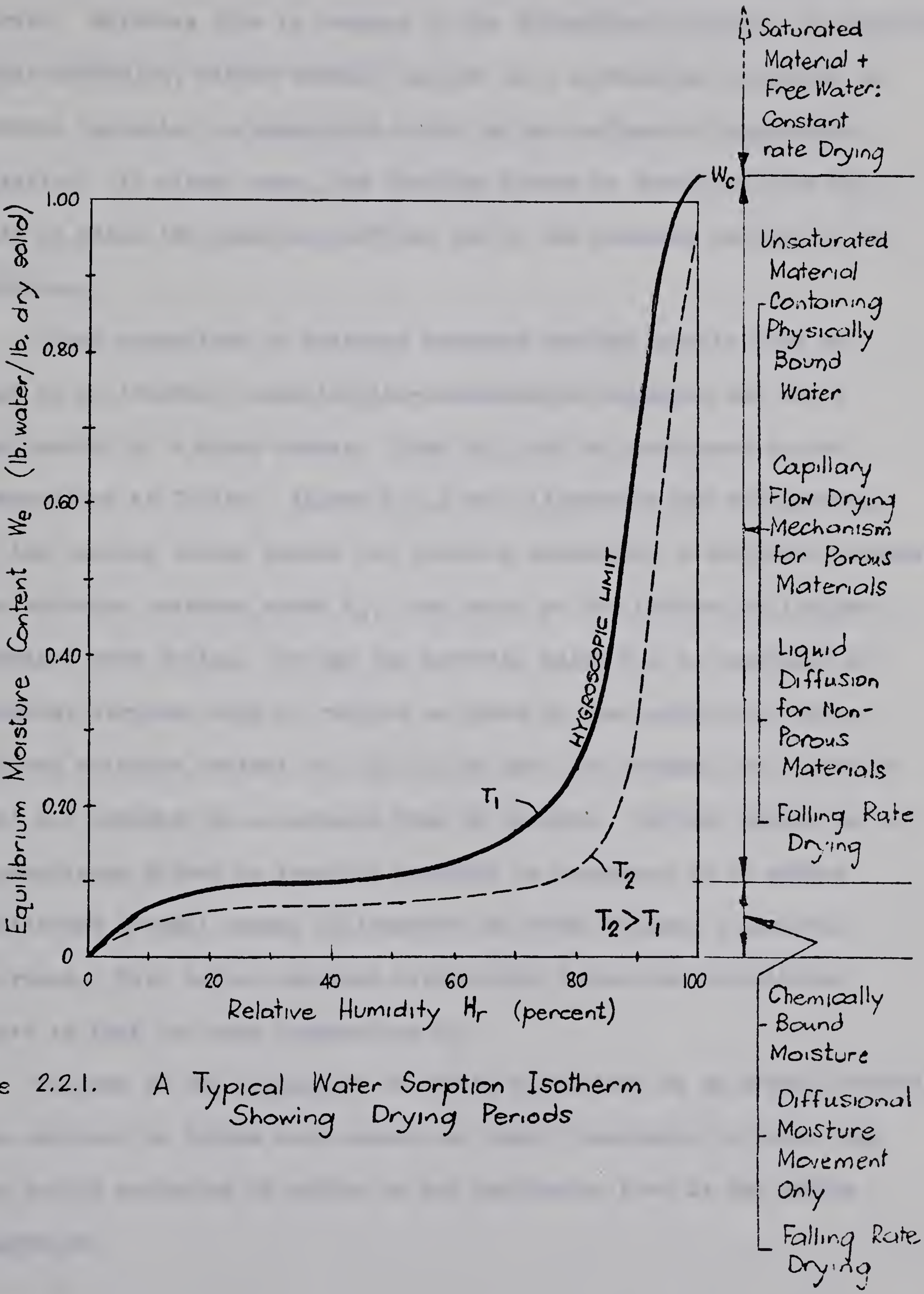

Figure 2.2.1. A Typical Water Sorption Isotherm Showing Drying Periods

Non-porous substances will not exhibit a capillary-flow drying period. Moisture flow is reduced to the diffusional movement of individual water molecules, either between defects in a crystalline structure or between vacancies in adsorption sites on the surfaces of hygroscopic material. In either case, the limiting factor in drying will be the rate at which the molecules diffuse out of the external surface of the material.

Other mechanisms of moisture movement include gravity flow and flow by an internal vapourization-condensation sequence, but these are usually of a minor nature. They will not be considered in the discussions to follow. Figure 2.2.1 will illustrate the relationship of the various drying phases and possible mechanisms of moisture movement. For moisture contents above W_c, free water at the surface will allow constant rate drying. To dry the material below W_c, air humidity at external surfaces must be reduced as shown by the equilibrium curve. A final moisture content of 0.10 lb./lb.dry, for example, will require that air humidity be no greater than 40 percent. Further drying may be accomplished either by reducing humidity as necessary or by adding sufficient thermal energy to liberate the water without a humidity decrease. This latter approach effectively lowers the equilibrium curve to that for some temperature T_2.

Because of the complexity of drying mechanisms in an actual material, the analysis to follow will assume an 'ideal' substance in which only one drying mechanism is active at any particular time in the drying operation.

3. ANALYSIS OF A MICROWAVE DRYING SYSTEM

3.1 Microwave Aspects of Drying

At microwave frequencies, electromagnetic energy is absorbed in molecular dielectric materials through the motion of dielectric molecules in response to applied fields. The motion consists of a distortion of the electronic structure of each atom of the material, a distortion of molecular structure by bond angle and interatomic spacing changes, and, for polar molecules, a tendency of the dipole to align itself with the applied field. As the various particles are accelerated by the fields, they emit radiation which is absorbed by neighbouring particles as thermal energy.

At very low applied field frequencies for constant field conditions, the molecule is subject to relatively small accelerations and very few reach sufficient values to emit thermal quanta. As field frequencies rise, the dipole motion, involving the largest inertial constants, begins to fall behind field oscillations. At this point, accelerations are large and dielectric losses correspondingly large. Eventually, beyond some frequency determined by the natural relaxation time τ_d of the dipoles, the molecules can no longer follow the field and orientational movements are reduced to small oscillations about a rest position. Dielectric losses drop to very low values and remain low until the exciting frequency approaches a resonance. In general, a rotational resonance will occur in the high microwave or low infrared regions of the spectrum. Water vapour, for example, has a very broad resonance with a maximum occurring at 22,300 MHz at 1 atmosphere pressure. The effects on dielectric losses of this resonance appear at frequencies as low as 100 MHz.

While the dissipative effects rise and pass through a first maximum, energy stored by the dielectric in the form of potential and kinetic energies of the molecular oscillators begins to fall as the frequency approaches $\frac{1}{2\pi\tau_d}$. The inability of the dipole to orient appreciably at frequencies beyond this results in the energy storing ability of the dielectric decreasing to a constant value generally well below the low frequency value.

Field theory relates the applied field $\bar{E}$ to the net dielectric response or electric displacement $\bar{D}$ through a parameter known as the permittivity ε of the material:

$$\bar{D} = \varepsilon\bar{E}$$

Although ε is often non-linear (dependent on $|\bar{E}|$ and $|\bar{H}|$), and non-isotropic (dependent on direction) in actual materials, simplifying assumptions of linearity and isotropy will be made for the following discussion. The former assumption is justified in dealing with most macroscopic matter at relatively low field strengths. In addition, bulk materials usually consist of molecules or molecular groups randomly oriented which result in an overall isotropic effect. For time harmonic fields, the permittivity is treated as a complex quantity $\varepsilon' - j\varepsilon''$. The displacement current, $\frac{\partial\bar{D}}{\partial\theta}$, now also complex, may be separated into an energy storing reactive component, $j\omega\varepsilon'\bar{E}$, out of phase with the applied field while dissipation effects are accounted for by an in-phase "conductive" component, $\omega\varepsilon''\bar{E}$. The following discussion will concern only dielectrics in which the true conduction current $\sigma\bar{E}$ is negligible in comparison to the dissipative component of displacement current $\omega\varepsilon''\bar{E}$. Results obtained under this assumption will be valid for most wet solid systems except for metallic solids or materials in concentrated brine (0.1N NaCl or greater) solutions. Because the

materials considered will be non-magnetic in general, the magnetic displacement current $\bar{M}$ is simply the free-space value

$$\bar{M} = \mu_o \frac{\partial \bar{H}}{\partial \theta} ,$$

$$\text{or} \quad \bar{M} = j\omega\mu_o \bar{H}$$

in complex notation, where magnetic losses are assumed to be zero.

The time-average power dissipated in a lossy material $\bar{P}_d$ may be calculated using

$$\bar{P}_d = \iiint_{\text{vol.}} \omega\varepsilon''|\bar{E}|^2 \, dv \qquad \ldots (3.1.1)$$

In order to evaluate $\bar{P}_d$, the variation of loss factor ε'' and field intensity $\bar{E}$ with position at the applied frequency ω must be known. Because of the relatively large loss factor of water at microwave frequencies, ε'' of a wet material, especially during later drying stages, may vary appreciably from place to place in the material. As a further complication, ε'' is a function of both temperature and frequency and will depend quite strongly on the material temperature distribution. Voss [23] gives an approximate empirical expression for the temperature dependence for water at a microwave frequency f:

$$T \tan \delta = 1.82(10^{-9})\, f - 1.2 \qquad \ldots (3.1.2)$$

where T = absolute temperature, °K, and $\tan \delta = \frac{\varepsilon''}{\varepsilon'}$. To obtain $\varepsilon''(T)$, it is necessary to have $\varepsilon'(T)$, which varies between

$$\varepsilon' = 80 - 0.4(T - 293)$$

for frequencies up to 10^8 Hz and temperatures between 0°C and 100 °C at 1 atmosphere, and

$$\varepsilon' = 87 - 0.36T \qquad \ldots (3.1.3)$$

over the same temperature range between frequencies of 2 and 3 GHz [11,23].

The variation of ε'' with moisture content in a system consisting

of a non-polar solid and water is given approximately by:

$$\varepsilon = \varepsilon_{ds} \left\{ 1 + \frac{3\left(\frac{W}{W + \rho_w/\rho_s}\right)}{\left(\frac{\varepsilon_w + 2\varepsilon_{ds}}{\varepsilon_w - \varepsilon_{ds}}\right) - \left(\frac{W}{W + \rho_w/\rho_s}\right)} \right\} \qquad \ldots (3.1.4)$$

where ε_{ds} = complex permittivity of the dry solid (farad/m)

ε_w = complex permittivity of water (farad/m)

W = moisture content (lb. water/lb. dry solid)

ρ_w = density of water (lb./ft.^{3})

ρ_s = absolute density of the dry solid (lb./ft.^{3})

This relation in a slightly different form was given by Lewin [12] in connection with prediction of the bulk dielectric constant of a particle-loaded dielectric. It is valid for situations in which the solvent (continuous phase) is non-polar while the particles (dispersed phase) may be polar if they are liquid. Use of the relation for wet solids requires the solid to be the continuous phase.

Substituting $\varepsilon = \varepsilon' - j\varepsilon''$ and assuming the dry solid to be lossless,

$$\varepsilon' = \frac{(1 - \tilde{R})(1 + 2\tilde{R})(\varepsilon_w'^2 + \varepsilon_w''^2) + (4 + \tilde{R} + 4\tilde{R}^2)\,\varepsilon_w'\varepsilon_{ds} + 2(1 - \tilde{R})(2 + \tilde{R})\varepsilon_{ds}^2}{[(1 - \tilde{R})\varepsilon_w' + (2 + \tilde{R})\varepsilon_{ds}]^2 + (1 - \tilde{R})^2\varepsilon_w''^2}$$

$$\varepsilon'' = \frac{9\tilde{R}\varepsilon_w''\,\varepsilon_{ds}^2}{[(1 - \tilde{R})\varepsilon_w' + (2 + \tilde{R})\varepsilon_{ds}]^2 + (1 - \tilde{R})^2\varepsilon_w''^2} \qquad \ldots (3.1.5)$$

where $R = \frac{W}{W + \rho_w/\rho_s}$.

It should be noted that any mixture in which the water is bound will exhibit a considerably different dielectric loss behavior than that given by (3.1.5). The loss due to water should decrease markedly as molecular movement is hindered by binding forces. For reference, the variation of

the complex dielectric constant components of water with temperature and frequency is given in Figure 3.1.1.

The variation of $\bar{E}$ throughout the dielectric must also be considered. For an unbounded lossy dielectric, the field $\bar{E}_t$ transmitted through the air/dielectric interface will be attenuated exponentially as it penetrates the material a distance z from the interface:

$$|\bar{E}_t|_z = |\bar{E}_t|_o \, e^{-\alpha_d z}$$

where α_d, the dielectric loss attenuation constant, is given by:

$$\alpha_d \simeq \frac{\omega}{2} \sqrt{\mu_o \varepsilon'} \tan\delta$$

if $\tan\delta \gg \frac{\sigma}{\omega\varepsilon'}$, and $\tan\delta \ll 1$. ... (3.1.6)

Extension to finite systems (guided waves) can be made by replacing ω in the above with $\omega\sqrt{1 - (f_c/f)^2}$. Not all of the field incident on the material surface enters the material, however. If the intrinsic impedance of the dielectric, η, defined by

$$\eta = \sqrt{\frac{\mu}{\varepsilon}}$$

is different from the impedance of free space, $\eta_o = 377$ ohms, only a fraction $\tilde{T}$ of the incident field will be transmitted:

$$\tilde{T} = \frac{E_t}{E_i} = \frac{2\eta}{\eta + \eta_o}$$

where, if dielectric losses are much greater than conduction losses, $(\tan\delta \gg \frac{\sigma}{\omega\varepsilon'})$,

$$\eta \simeq \sqrt{\frac{\mu_o}{\varepsilon'}} \left(1 + j \frac{\tan\delta}{2}\right) \quad \text{... (3.1.7)}$$

The variation of $\bar{E}_t$ over x-y planes, depending both on drier configuration and on dielectric property x-y variation, is too much a function of the specific drying system to be amenable to useful generalization within the scope of this study. Consequently, materials will be

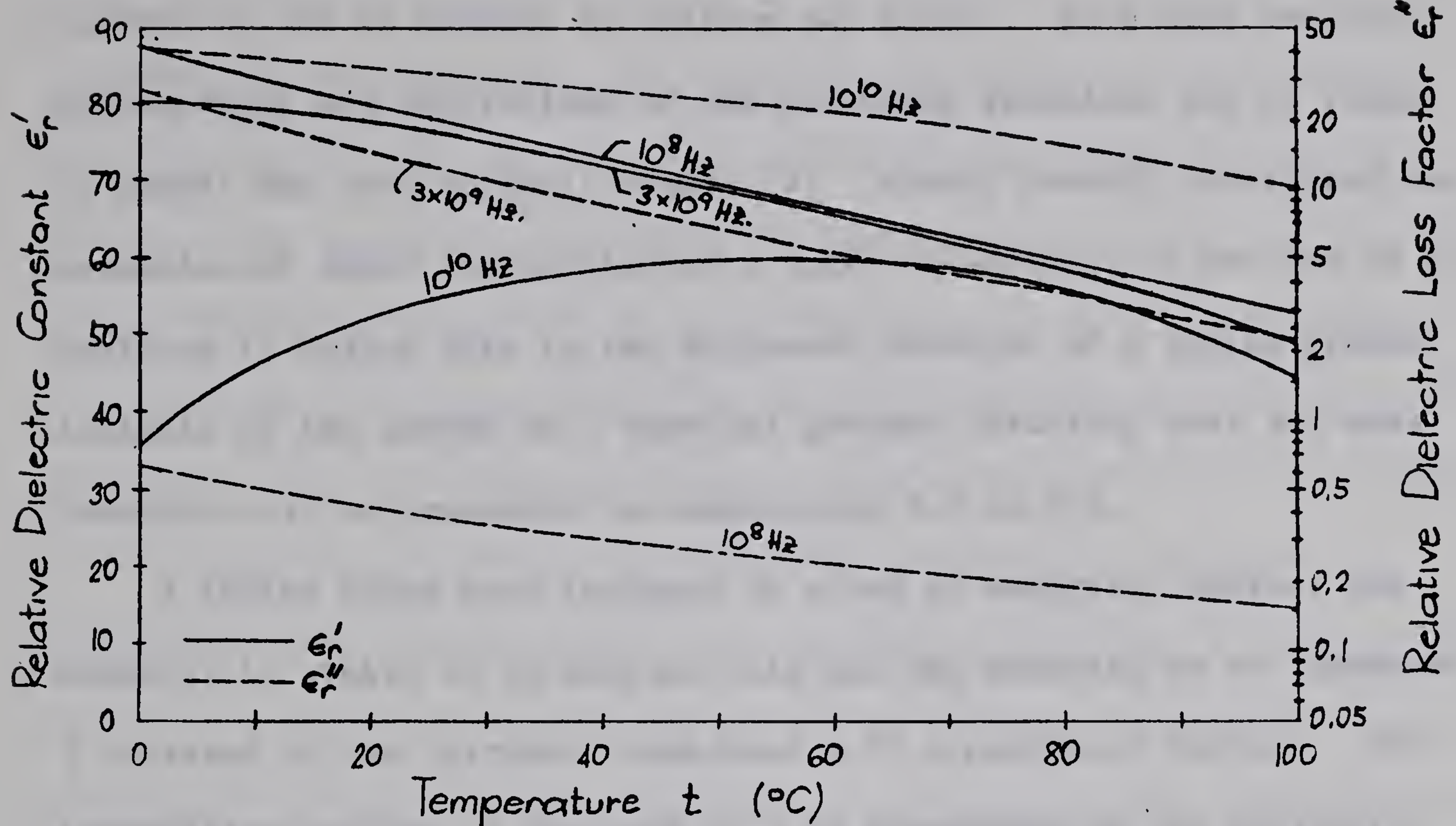

Figure 3.1.1. Complex Permittivity of Water as a Function of Temperature and Frequency [21]

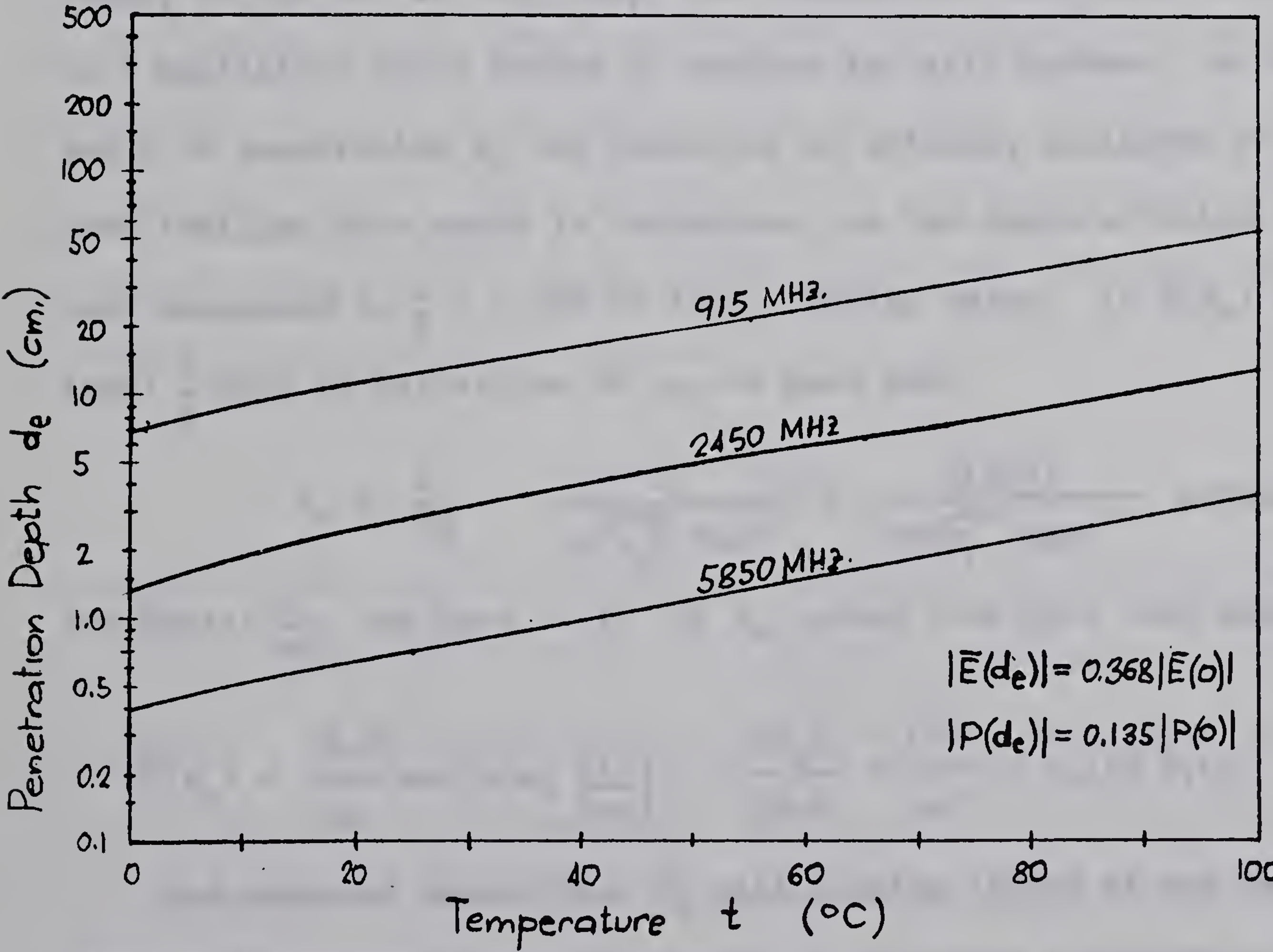

Figure 3.1.2. Variation in Field Penetration Depth d_e for Water

assumed to lie in regions of uniform x-y fields. Both more detailed explanations and derivations of the preceding relations may be found in almost any text on field theory [7]. Having briefly considered the mechanism of power dissipation in a lossy dielectric, we are now in a position to relate this to the microwave behavior of a drying system. Analysis of the system as a physical process involving heat and mass transfer will be presented in subsections 3.2 to 3.4.

A finite plane wave incident on a bed of material, whether the material is static or in motion, will see the material as an impedance Z (related to the intrinsic impedance η by a geometric factor). The transmitted portion of the wave will be attenuated by the dielectric until it exits from the opposite bed surface. If the material is very lossy, or the bed is very deep, the transmitted wave will be attenuated to a negligible value before it reaches the exit surface. An effective depth of penetration d_e can therefore be defined, analogous to the more familiar skin depth in conductors, as the depth at which fields have decreased to $\frac{1}{e} = 0.368$ of their initial value. If $E(d_e)$ is to equal $\frac{1}{e}E(0)$ by definition of d_e, we must have

$$d_e = \frac{1}{\alpha_d} \approx \frac{2}{\omega\sqrt{\mu_o\varepsilon'}\ \tan\delta} = \frac{3(10^8)}{\pi f\sqrt{\varepsilon_r'}\ \tan\delta} \text{ meters} \qquad \ldots (3.1.8)$$

for $\tan\delta \gg \frac{\sigma}{\omega\varepsilon'}$, and $\tan\delta \ll 1$. In d_e, power flow will thus decrease to

$$\bar{\bar{P}}(d_e) = \frac{|E_o|^2}{2Z}\exp\left[-2\alpha_d\left(\frac{1}{\alpha_d}\right)\right] = \frac{|E_o|^2}{2Ze^2} = \frac{\bar{\bar{P}}(0)}{e^2} = 0.135\ \bar{\bar{P}}(0)$$

Bed material deeper than d_e will receive little of the benefit of dielectric heating: thermal conduction may become a significant factor in heat transfer. On the other hand, it is not particularly efficient to have the exit wave still carrying substantial power unless the system is such

that the wave can be re-directed into the material. Examples would be a resonant structure or a tunnel in which the wave is reflected at a suitable angle from top and bottom conductors as it passes down the tunnel. The latter would probably be ideal for a concurrent-flow drier: wet material would receive the highest power; dry material, the lowest.

Because ε is temperature, frequency and material dependent, d_e will similarly vary with these conditions. Within the material restrictions noted previously, d_e will have a minimum value for the ambient temperature wet feed material; this minimum will always be greater than that for water alone in the same geometry (Figure 3.1.2). Thus, bed depth will normally be chosen greater than $(d_e)_{\text{initial}}$ to give acceptable power dissipation near the lowest moisture contents to be encountered. Since the variation of d_e with temperature (or time) will determine, unless some critical drying characteristic overrides, the maximum practical bed depth, it is of considerable importance that the behavior of this parameter be known. The penetration depth can be calculated using either measured values of $\varepsilon(T)$ and equation 3.1.8 or directly from the propagation constant $\gamma_2(T)$ of the wet material:

$$d_e = \frac{1}{\alpha} = \frac{1}{\mathrm{Re}\{\gamma_2\}} \qquad \ldots(3.1.9)$$

Conductor losses have been neglected since they will be small compared to dielectric losses in drying applications. The change in d_e with moisture content is not particularly important in cases in which the unabsorbed power flow at low moisture content is always fed back into the material until reduced to a negligible amount.

Because dielectric losses are largest at low temperatures where thermal motion of the dipoles does not interfere as much with response to applied fields, d_e will be least at the lowest material temperature

expected. For most purposes, this can be taken as the temperature of the wet feed material, so that $(d_e)_{min}$ will be given for t_{min} and W_{max}. For a given feed material, $(d_e)_{min}$ will depend only on frequency: decreasing f will increase d_e. However, decreasing f will also decrease $\bar{P}_d$ and increase conductor losses. A basis on which to compromise between power density and penetration depth requirements is given in Section 3.5.

In order to estimate transmission coefficients, power densities and drier input impedance as drying proceeds, it will be necessary to know $\varepsilon(W,t)$ over the range of moisture content to be encountered and at several temperatures. While (3.1.2), (3.1.3) and (3.1.4) can be used in many cases for a rough value of ε, practical system design will require more accurate values. The method of Roberts and von Hippel [22] can be used to measure ε at constant temperature as a function of moisture content.

Several possible system configurations are illustrated in Figure 3.1.3. In the first, detector output would be kept at some very small value by automatic decrease of the microwave generator output. Faster drying would be possible only with additional meanders. A similar control system would be necessary in the tunnel drier to effect maximum power transfer. For both systems, the generator would be feeding a very nearly matched load since in the first case, reflections should be negligible, and in the second, reflections will be absorbed by the material. Maintaining detector output near zero will eliminate end reflections. The use of a resonant cavity is shown for a batch-type drier although it could equally well be adapted to continuous feed. Retuning of the cavity, necessary as the material permittivity changes, can be done in various ways depending upon the method of coupling to the cavity [2].

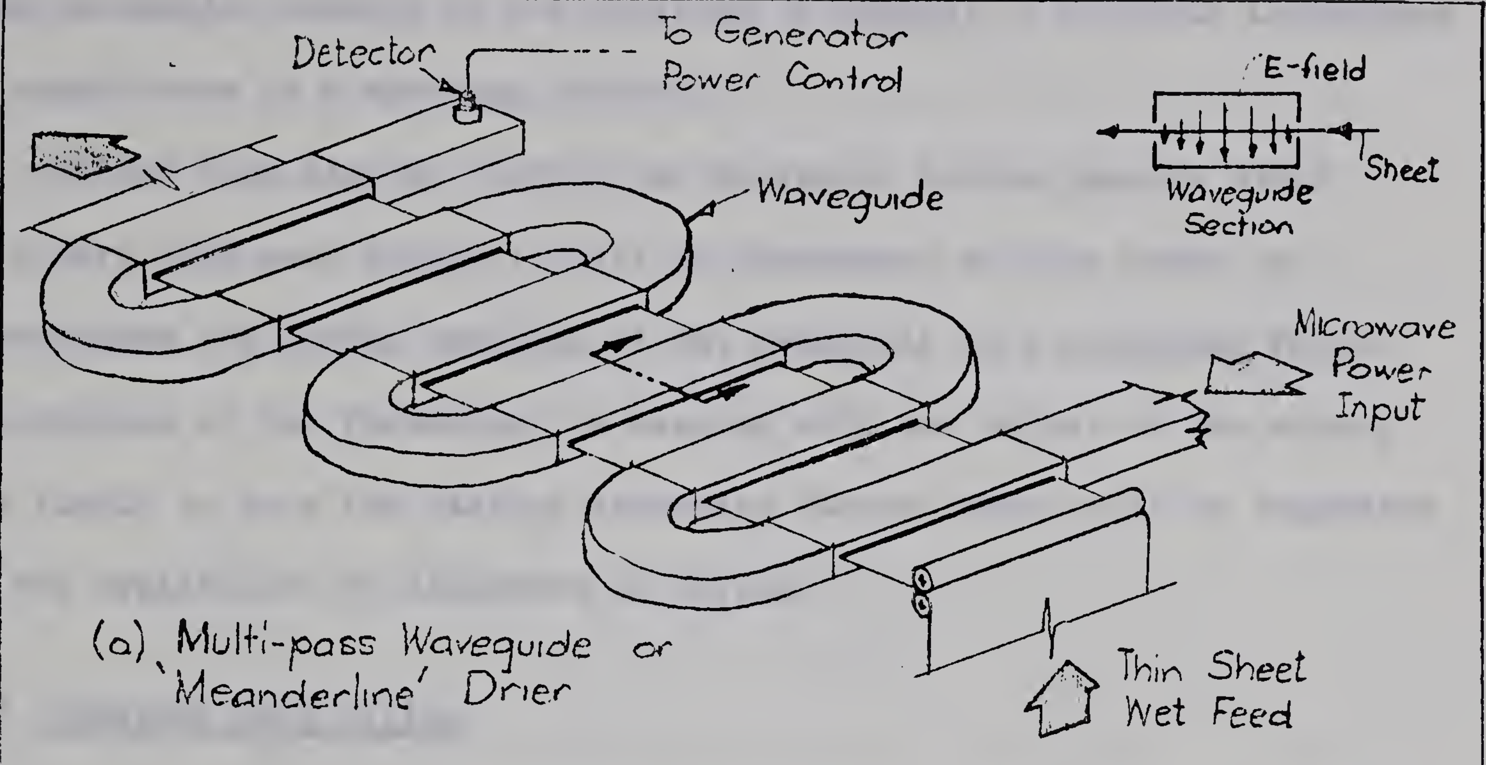
Detector
To Generator
Power Control
E-field
Sheet
Waveguide Section
Waveguide
Microwave
Power
Input
Thin Sheet
Wet Feed

(a) Multi-pass Waveguide or 'Meanderline' Drier

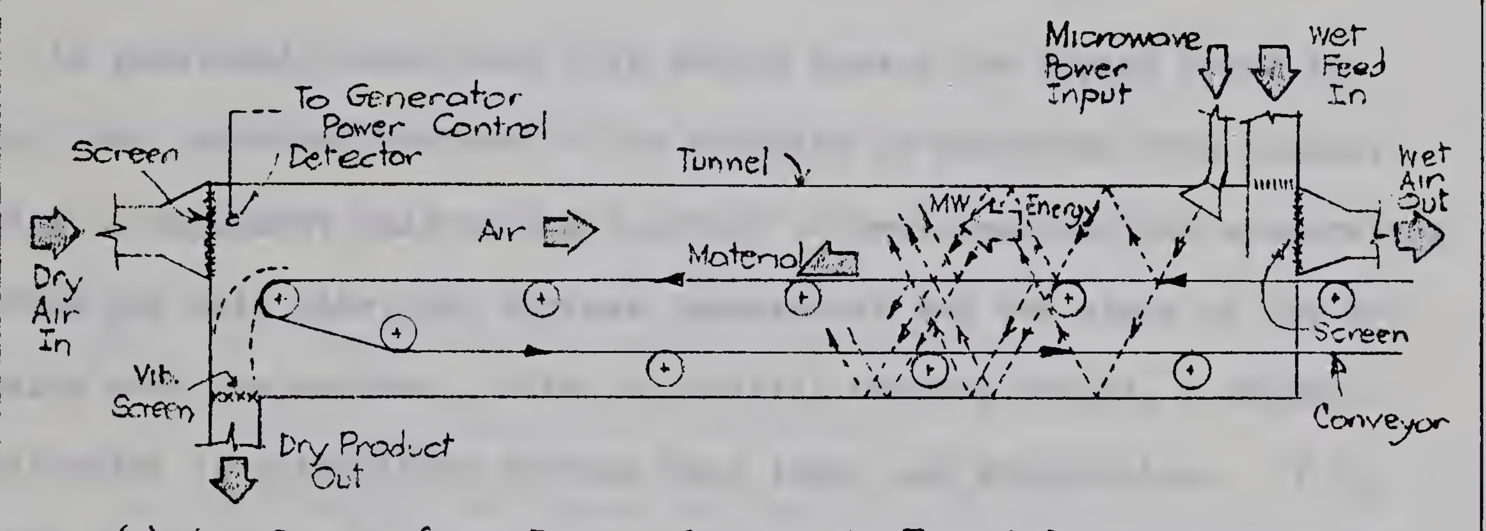
Microwave
Power
Input
Wet
Feed
In
To Generator
Power Control
Detector
Screen
Tunnel
Wet
Air
Out
Dry
Air
In
Air
Material
MW
Energy
Screen
Vib.
Screen
Conveyor
Dry Product
Out

(b) Air Counter-flow, Energy Concurrent Tunnel Drier

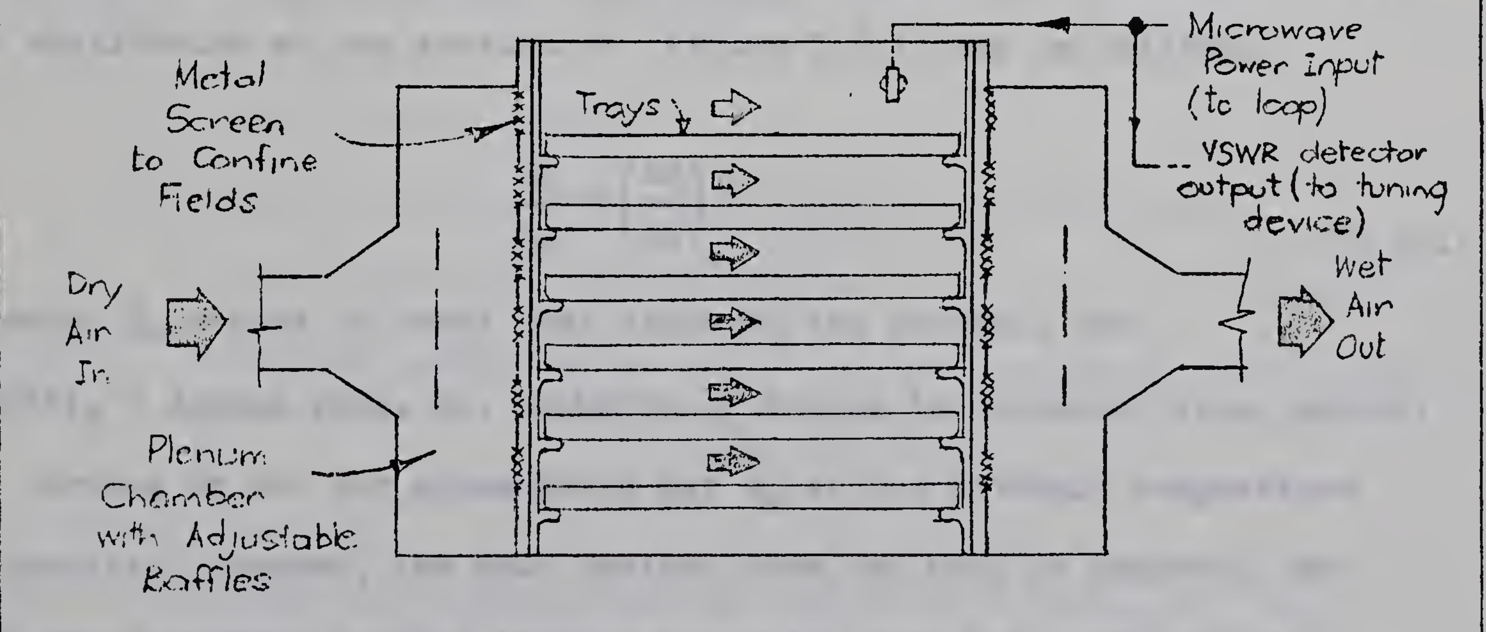
Metal
Screen
to Confine
Fields
Trays
Microwave
Power Input
(to loop)
VSWR detector
output (to tuning
device)
Dry
Air
In
Wet
Air
Out
Plenum
Chamber
with Adjustable
Baffles

(c) Multi-mode Resonant Cavity Tray Drier

Figure 3.1.3 Typical Microwave Drier Configurations

Tuning will in general be varied to maintain minimum VSWR in the power feed waveguide, usually by the addition or removal of suitable inductance or capacitance in a matching network.

Rather than discuss further the microwave system details which will vary with each drier, it will be convenient at this point to investigate the drying behavior of wet materials in a microwave field. The purpose of the foregoing, in keeping with the object of the study, was simply to note the various microwave factors which will be important to the application of microwave in drying.

3.2 Constant Rate Drying

As previously described, this period covers the drying phase in which the external surface of the material is saturated with liquid. Drying is dependent only on the quantity of heat reaching the evaporating surface per unit time, the surface temperature and the state of the air passing over the surface. After an initial warm-up period, a dynamic equilibrium is established between heat input and evaporation. If λ_s is the latent heat of vapourization at the true surface temperature t_s, the equilibrium at any section dx (Figure 3.2.1) may be written:

$$\frac{\overset{o}{q}_t}{\lambda_s} = \left(\frac{dw}{d\theta}\right)_c \qquad \ldots (3.2.1)$$

in which $\overset{o}{q}_t$ = rate of total heat input to the surface, and $(dw/d\theta)_c$ = drying rate, lb. water/hr., during the constant rate period.

Drying by hot air alone would put t_s at the wet-bulb temperature of the air. However, the heat derived from the body of material and from other sources such as thermal radiation from hot surfaces will cause a deviation from adiabatic conditions with the result that t_s will

be in general considerably higher than the wet-bulb temperature. This would be expected since the higher rate of evaporation must be caused by a larger mass transfer driving potential (usually taken as the vapour pressure difference between surface film air and distant air). For a general case of the drying of a granular solid, Marshall and Hougen [15] developed an empirical relation for evaporation under constant-rate conditions:

$$\left(\frac{dw}{d\theta}\right)_c = K_G \left(\frac{D_p G}{\mu}\right)^n \left(\frac{\mu}{\rho_f \tilde{D}_v}\right)^m \left(\frac{p_T}{p_{fm}}\right) \Delta p_w \qquad \ldots (3.2.2)$$

where: K_G = mass transfer coefficient (lb./hr. ft.^{2} atm.)

D_p = average particle diameter (ft.)

G = mass velocity of the air stream (lb./hr. ft.^{2})

μ = dynamic viscosity of the air film (lb./hr. ft.)

$\left(\frac{D_p G}{\mu}\right)$ = modified Reynold's number, dimensionless

ρ_f = density of the air film (lb./ft.^{3})

$\tilde{D}_v$ = diffusivity of vapour through air (ft.^{2}/hr.)

$\left(\frac{\mu}{\rho_f \tilde{D}}\right)$ = Schmidt number, dimensionless

p_T = total pressure (atm.)

n,m = experimentally determined exponents, dimensionless

p_{fm} = logarithmic mean partial pressure of dry air in the boundary film

$$= \left[\frac{(\text{surface partial press. } p_{fs}) - (\text{upper boundary partial press. } p_{ft})}{\ln (p_{fs}/p_{ft})}\right]$$

$\Delta p_w = p_{ws} - p_{wa}$

= difference between partial pressures of vapour at the particle surface and vapour in the main air stream (atm.)

While the above relation demonstrates the physical quantities of importance

in limiting the rate at which water vapour can be transferred from surface film to main air stream, some simplification is possible for an air/water system.

For a given system, D_p will be constant if material shrinkage is neglected, and the Schmidt number is nearly independent of temperature ($\mu \propto T^{1/2}$, $\tilde{D} \propto T^{3/2}$, $p_{fm} \propto T^{-1}$); these quantities can be absorbed into a modified mass transfer coefficient K'_G. The usual assumption that $p_{fm} \simeq p_T$, made for the humidities and temperatures encountered in normal drying systems, cannot be made in general for microwave driers. Since heat transfer is not primarily dependent on a temperature difference between air and material, it may be of advantage to increase the surface temperature to a limit dictated by quality considerations or to as near boiling as possible. The ratio $\left(\frac{p_T}{p_{fm}}\right)$ is then, for $p_T = 1$ atm.:

$$\left(\frac{1}{p_{fm}}\right) = \frac{\ln\left(\frac{1}{1 - p_{ws}}\right)}{p_{ws}} \qquad \ldots (3.2.3)$$

since $p_{ft} \simeq p_T$ for sufficiently high air velocities, and $p_{fs} = 1 - p_{ws}$.

In terms of absolute humidity H,

$$p_w = p_{fm}\left(\frac{M_a}{M_w}\right)H = \frac{(1 - p_w)}{0.622}H = \frac{1}{1 + \frac{0.622}{H}} \qquad \ldots (3.2.4)$$

so that:

$$\Delta p_w = \frac{\Delta H}{0.622\left(1 + \frac{H}{0.622}\right)^2} \quad \text{(atm.)} \qquad \ldots (3.2.5)$$

Flow patterns in the drying chamber appear to have the greatest effect on the exponent n: for flow parallel to a plane surface, it is usually given as 0.8 while for flow directed perpendicular to the drying

surface, 0.37. Because $\left(\frac{1}{\mu}\right)^n$ is proportional to $T^{-n/2}$, it will vary slowly with temperature, approximately $0.002\left(\frac{n}{2}\right)$ per cent per °R. Consequently, $\left(\frac{1}{\mu}\right)^n$ can be considered temperature independent and included in K'_G also. Equation (3.2.2) can now be reduced to:

$$\left(\frac{dw}{d\theta}\right)_c \simeq K'_G \; G^n \left[\frac{-\ln\,(1 - p_{ws})}{p_{ws}}\right] \left[\frac{1}{0.622 \quad 1 + \frac{H_m}{0.622}^{\,2}}\right] \Delta H$$

$$\simeq K' \left[\frac{-\ln\,(1 - p_{ws})}{p_{ws}}\right] (H_s - H_a) \qquad \ldots (3.2.6)$$

where $K' = \left(\frac{K'_G}{0.622}\right) G^n$ and the logarithmic mean humidity $H_m = \frac{H_s - H_a}{\ln(H_s/H_a)} \ll 1$ for $H_s \gg H_a$.

The drying rate associated with convective heat transfer from the air stream is generally given in a form similar to (3.2.2):

$$\left(\frac{dw}{d\theta}\right)_c = \left[\frac{a\; G^n\; A}{\lambda_s}\right] (t_a - t_s) = h_c \left(\frac{A}{\lambda_s}\right) (t_a - t_s) \qquad \ldots (3.2.7)$$

where: a = a constant (0.128 for air flow parallel to the surface, 0.37 for flow perpendicular to the surface [13])

n = 0.37 to 0.8, as before

A = evaporating surface area (ft.^{2})

h_c = convective heat transfer coefficient (BTU/ft.^{2} hr. °F)

t_a = airstream temperature (dry bulb) (°F)

In many cases, heat will reach the evaporating surface by means of conduction through the container and material and by means of thermal radiation from the hot walls of the drier. Shepherd et al [18] have

derived a correction for these effects assuming container and drier walls are at the temperature t_a and that convective heat transfer coefficients for the container walls and for the liquid surface are equal:

$$h_t' = (h_c + h_r)\left\{1 + \frac{A_u}{1 + \dfrac{d\,(h_c + h_r)}{k_T}}\right\} \qquad \ldots (3.2.8)$$

where: h_t' = total heat transfer coefficient (BTU/hr. ft.^{2} °F)

h_r = radiative heat transfer coefficient (the calculation of this is rather involved and can be obtained from Perry [17], Section 10-10)

A_u = ratio of outside unwetted surface to evaporating surface

d = bed depth (ft.)

k_T = thermal conductivity of the wet material (BTU/ft. °F hr.)

The resulting drying rate for convection, conduction and thermal radiation is:

$$\left(\frac{dw}{d\theta}\right)_{ct} = h_t'\left(\frac{A}{\lambda_s}\right)(t_a - t_s) \qquad \ldots (3.2.9)$$

The microwave contribution to drying can be determined by first integrating the heat equation with a source field $\Pi(x,y,z,\theta)$ watts/m^3 (or Π' BTU/hr. ft.^{3}) to obtain the temperature distribution. For constant c, ρ and k_T:

$$c\rho\,\frac{\partial t}{\partial\theta} = k_T\nabla^2 t + \Pi' \qquad \ldots (3.2.10)$$

where: c = specific heat of the wet material (BTU/lb. °F)

ρ = wet material density (lb. mass/ft.^{3})

k_T = thermal conductivity (BTU/ft. hr. °F)

Π' = power density = $\dfrac{\partial\bar{P}_d'}{\partial v}$ (BTU/hr. ft.^{3})

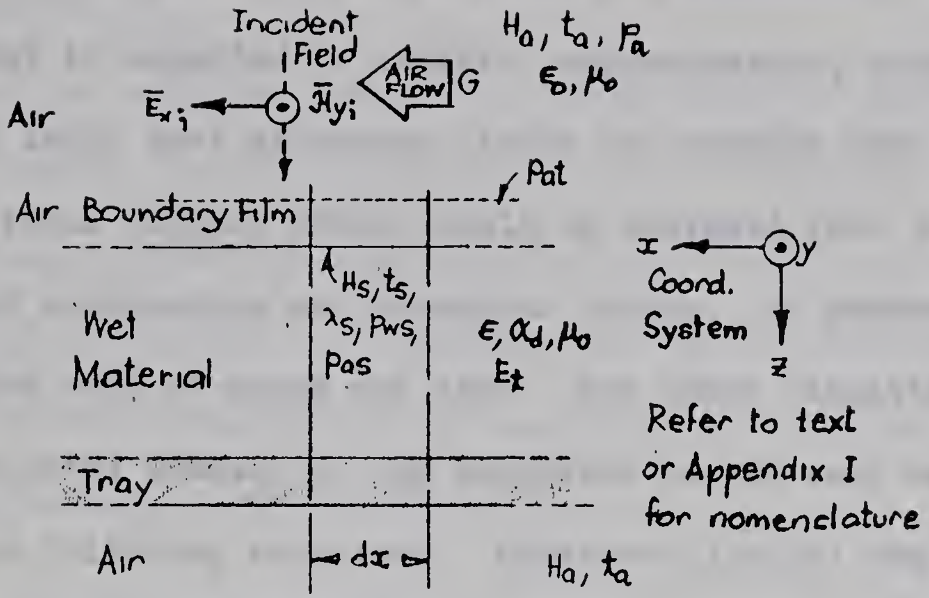
Incident Field
H_a, t_a, P_a
ϵ_0, μ_0
Air
$\bar{E}_{x_i}$
$\bar{H}_{y_i}$
AIR FLOW
G
Pat
Air Boundary Film
x
y
Coord. System
z
Wet Material
$H_s, t_s, \lambda_s, p_{ws}, P_{as}$
$\epsilon, \alpha_d, \mu_0$
E_t
Refer to text or Appendix I for nomenclature
Tray
Air
dx
H_a, t_a

Figure 3.2.1 Constant Rate Drying Model

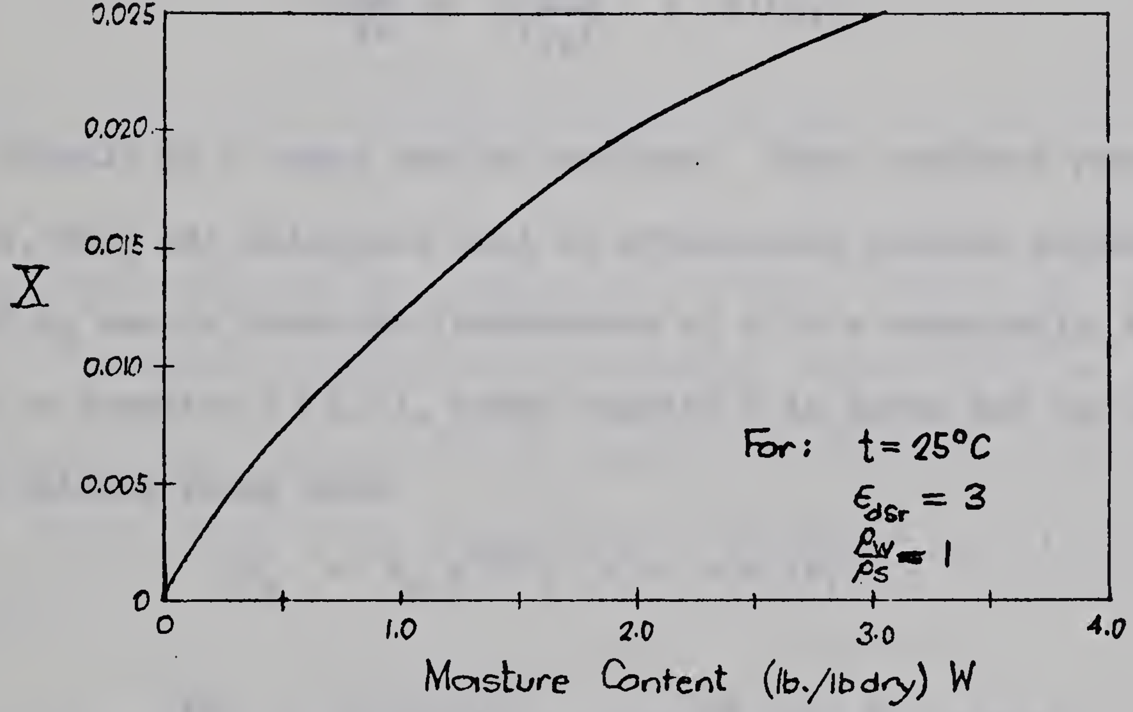

Figure 3.2.2 The Moisture Content Dependence of Power Density $\Pi = \Pi_0 X(W)$, where Π_0 is a constant.

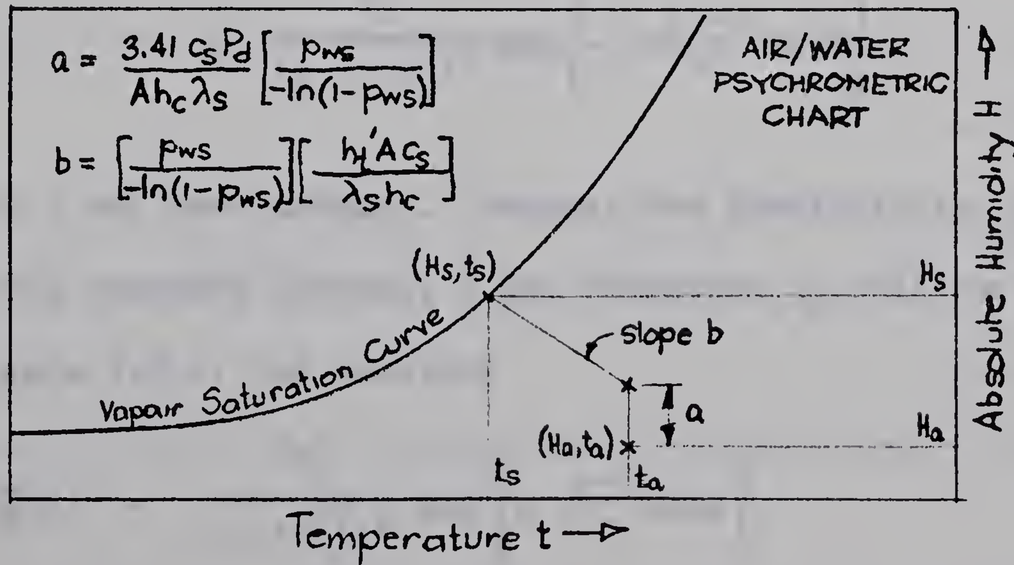

Figure 3.2.3 Determination of Surface Temperature and Humidity

For many drying situations, the material temperature can be assumed uniform over a horizontal plane if edge effects are neglected. Moisture content can similarly be expected to exhibit, approximately, only a z-dependence. Both imply that microwave fields are uniform over the bed surface, a desirable feature which should be designed into any drier to prevent localized overheating and irregular drying. In general, then, $\bar{E}_t$ will be a function only of depth and time. For other situations, an average $\bar{E}_t$ based on modes present in the enclosure can be used as an approximation in the following relations. Equation (3.2.10) may therefore be reduced to its one-dimensional form:

$$c\rho\frac{\partial t}{\partial\theta} = k_T\frac{\partial^2 t}{\partial z^2} + \Pi'(z,\theta) \qquad \ldots (3.2.11)$$

The details of Π' must now be resolved. Under constant rate drying conditions, many wet materials will be effectively uniform mixtures and both ε and α_d can be taken as independent of z to a reasonable approximation. Referring to equation (3.1.1), power density Π is given for the simplest case of a uniform plane wave

$$E_x = E_o\, e^{-\gamma z}, \quad \gamma = \alpha + j\beta,$$

by:

$$\Pi = \frac{\partial\bar{P}_d}{\partial v} = \omega\varepsilon''|E_t|^2 = \omega\varepsilon'' E_o{}^2\left|\frac{2\eta}{\eta + \eta_o}\right|^2 e^{-2\alpha_d z}$$

$$\simeq \omega\varepsilon''\frac{E_o^2}{(1+\sqrt{\varepsilon_r'})^2}\exp\left[-\,\omega\sqrt{\mu_o\varepsilon'}\,\tan\delta\right] \qquad \ldots (3.1.12)$$

in which $\frac{1}{4}\tan^2\delta \ll 1$ has been assumed. Because the permittivity of wet material varies with moisture content, ε and therefore α_d will be time dependent. In Figure 3.2.2, the quantity

$$\overline{\underline{X}}(W) = \frac{\varepsilon_r''}{(1+\sqrt{\varepsilon_r'})^2}\exp\left[-\sqrt{\varepsilon_r'}\,\tan\delta\right]$$

where $\Pi = \Pi_0 \, \overline{\underline{X}}(W)$, and

$$\Pi_0 = \omega\varepsilon_0 E_0^2 \exp\left[\omega\sqrt{\mu_0\varepsilon_0}\right],$$

has been plotted against moisture content to demonstrate the magnitude of the variation. Because of the strong dependence of Π on moisture content, material temperature will vary substantially with W and, therefore, time during falling rate drying. For moderate and low drying rates, equation (3.2.11) may be evaluated over a time interval $\Delta\theta$ within which Π does not vary appreciably. Setting $\frac{\partial t}{\partial \theta} = 0$:

$$\frac{d^2t}{dz^2} = -\frac{0.0966\omega\varepsilon'' E_0^2}{k_T\,(\sqrt{\varepsilon_r'} + 1)^2}\, e^{-2\alpha_d z} \qquad \ldots (3.2.13)$$

so that $$(t - t_s)_{\Delta\theta} = \frac{0.0966\omega\varepsilon'' E_0^2}{4\alpha_d^2\, k_T\,(\sqrt{\varepsilon_r'} + 1)^2}\left[1 - e^{-2\alpha_d z} - 2\alpha_d z e^{-2\alpha_d d}\right] \qquad \ldots (3.2.14)$$

under the conditions that $\frac{dt}{dz} = 0$ for $z = d$, the bed depth, and $t = t_s$ at $z = 0$. A material container of low thermal conductivity has been assumed which is in keeping with the nature of practical microwave drier materials (see Section 5.1). The maximum temperature in the bed t_M will be given by:

$$(t_M - t_s)_{\Delta\theta} = \frac{0.0966\omega\varepsilon'' E_0^2}{4\alpha_d^2\, k_T\,(\sqrt{\varepsilon_r'} + 1)^2}\left[1 - (1 + 2\alpha_d d)e^{-2\alpha_d d}\right] \quad (F^\circ) \qquad \ldots (3.2.15)$$

and the mean temperature t_m for use in calculating average bed properties will be:

$$(t_m)_{\Delta\theta} = t_s + \frac{0.0966\omega\varepsilon'' E_0^2}{4k_T\alpha_d^2(\sqrt{\varepsilon_r'} + 1)^2}\left\{1 - \frac{1 - e^{-2\alpha_d d}}{2\alpha_d d} - d\alpha_d e^{-2\alpha_d d}\right\} \quad (^\circ F) \qquad \ldots (3.2.16)$$

It is now possible to equate mass transfer and total heat input rates:

$$AK' \left[\frac{-\ln(1 - p_{ws})}{p_{ws}}\right](H_s - H_a) \simeq \left(\frac{h_t' A}{\lambda_s}\right)(t_a - t_s) + \frac{3.41(\bar{P}_d)_{\Delta\theta}}{\lambda_s} \qquad \ldots (3.2.17)$$

where 1 watt = 3.41 $\frac{BTU}{hr}$. A ratio $\frac{h_c}{K'c_s}$, known as the psychrometric ratio, may be employed to remove K' from the rate balance equation. Experimentally, it is found that $\frac{h_c}{K'c_s} \simeq 1$ for air/water systems for relatively low humidities [Perry p. 15-2]. The validity of this relation should be unaffected by the presence of an independent heat source within the material: h_c, K' and c_s are functions only of the nature of the air/water interface, the air flow characteristics, air thermal conductivity, air and vapour specific heats, vapour diffusivity in air, and air viscosity. The microwave fields will have negligible effect on such variables. Replacing K' in equation (3.2.17),

$$(H_s - H_a) \simeq \left[\frac{h_t' c_s}{\lambda_s h_c}(t_a - t_s) + \frac{3.41\, c_s(\bar{P}_d)_{\Delta\theta}}{A h_c \lambda_s}\right]\left[\frac{p_{ws}}{-\ln(1 - p_{ws})}\right] \qquad \ldots (3.2.18)$$

For a given system, the quantities H_a, h_t', A, h_c, t_a and $\bar{P}_d$ are known or can be calculated. A trial value of t_s can be used to obtain initial values for p_{ws}, λ_s and c_s. H_s and t_s can be obtained from a psychrometric chart as shown in Figure 3.2.3.

Once H_s or t_s is known, the initial drying rate can be calculated directly using:

$$\left(\frac{dw}{d\theta}\right)_c = \left(\frac{h_t' A}{\lambda_s}\right)(t_a - t_s) + 3.41\,\frac{(\bar{P}_d)_{\Delta\theta}}{\lambda_s} \qquad \ldots (3.2.19)$$

If appreciable heat is being drawn from the air, the temperature t_a will vary across the bed length x_o. The outlet temperature t_2, as given by Perry, is:

$$t_2 = t_s + (t_1 - t_s) \exp \{-x_o h_t / G D_c c_s\}$$

where D_c is an effective flow channel diameter (ft.), usually taken as four times the channel cross-sectional area divided by the perimeter, and t_1 is the drier inlet air temperature (°F). A more accurate drying rate estimate can be obtained using the logarithmic mean temperature difference $(t_a - t_s)_m$, in equation (3.2.19) where:

$$(t_a - t_s)_m = \frac{t_2 - t_1}{\ln\left[\dfrac{t_2 - t_s}{t_1 - t_s}\right]} \qquad \ldots (3.2.20)$$

Constant rate drying time can then be estimated as a sum of n suitably short periods:

$$\theta_c = \sum_{i=0}^{n} \frac{(W_{i+1} - W_i)\lambda_{si}}{h_t'(t_a - t_s)_{mi} A + 3.41(\bar{P}_d)_i} \qquad \ldots (3.2.21)$$

where: W_o = initial moisture content

W_n = critical moisture content (beginning of falling rate period)

$(\bar{P}_d)_i$ = average microwave power input (watts) between time θ_i and $\theta + \Delta\theta$ such that $n\Delta\theta = \theta_c$.

3.3 Diffusion-Controlled Drying of Non-Porous and Hygroscopic Materials

Because of the complexity of diffusional phenomena, very few practical diffusion-controlled drying systems have been described satisfactorily from a theoretical basis. Much of the difficulty lies in the fact that the diffusivity $\tilde{D}$, a parameter characterizing the resistance to mass transfer on a molecular scale, varies with moisture content, temperature, humidity, structure and hygroscopic nature of the solid as well as bed geometry. Solution of the diffusion equation

$$\frac{\partial W}{\partial \theta} = \tilde{D} \frac{\partial^2 W}{\partial z^2} \qquad \ldots (3.3.1)$$

where $\tilde{D}$ = diffusivity of water (ft.^{2}/hr.), has been investigated in detail by Crank [3], among others, who has summarized many of the mathematical techniques necessary to obtain solutions for variable diffusivity. The constant diffusivity solution for a thin slab drying from one side,

$$\frac{W - W_e}{W_o - W_e} = \frac{8}{\pi^2}\left[e^{-a\theta} + \frac{1}{9}e^{-9a\theta} + \frac{1}{25}e^{-25a\theta} + \ldots\right] \quad \ldots (3.3.2)$$

where $a = \left(\frac{\pi}{2d}\right)^2 \tilde{D}$

d = slab thickness,

often used in connection with the analysis of diffusion-controlled drying, fails to give even qualitatively accurate results in all but the simplest of drying situations.

It appears that the use of a moisture gradient $\frac{dW}{dz}$ as the diffusional driving force is not completely justified in view of work reported by Babbitt [1] in which he was able to obtain moisture flow against the concentration gradient. If the evaporating surface of a bed is heated while the opposite (sealed) surface is cooled, a situation can be established in which a positive moisture content gradient and a negative vapour pressure gradient are present simultaneously. That this is possible can be shown by differentiation of an empirical sorption (equilibrium moisture content vs. relative humidity) relationship proposed by Henderson [8]:

$$W^B = \frac{\ln(1 - p_w/p_o)}{-CT} \quad \ldots (3.3.3)$$

where B and C are empirical constants

p_o = saturation vapour pressure at temperature T

p_w = actual vapour pressure at T

p_w/p_o = fractional relative humidity.

The differentiation yields:

$$\frac{dp_w}{dz} = \left[BCT\ (p_o - p_w)\ W^{B-1} \right] \frac{dW}{dz} + \left[C\ (p_o - p_w)\ W^{B} \right] \frac{dT}{dz} \qquad \ldots (3.3.4)$$

For a large enough negative $\frac{dT}{dz}$, $\frac{dp_w}{dz}$ will become negative and give rise to the conditions under which Babbitt noted his flow reversal. No general agreement is evident in the literature as to which is the correct choice of a driving force so that, on the basis of the preceding comments, a vapour pressure gradient will be assumed to govern diffusional liquid moisture movement.

Van Arsdel [19] has provided a means of introducing $\frac{dp_w}{dz}$ into the analysis through the use of a moisture permeability parameter Y:

$$\frac{\bar{w}_s}{A} \frac{dW}{d\theta} = G_w = - Y \frac{dp_w}{dz} \qquad \ldots (3.3.5)$$

where G_w = diffusional mass flow rate of water (lb./hr.ft.^{2})

Y = moisture permeability (lb./hr.ft.atm.)

$\bar{w}_s$ = dry solid weight (lb. dry)

A = bed or mass transfer surface area (ft.^{2}).

The permeability is related to diffusivity by:

$$Y \frac{dp_w}{dW} = \rho_s \tilde{D} \qquad \ldots (3.3.6)$$

where $\frac{dp_w}{dW}$ = slope of a water vapour pressure isotherm (atm./lb.water/lb.dry solid), such as equation (3.3.3).

In the absence of an internal temperature gradient, moisture distribution $W(z,\theta)$ and rate of moisture movement $G_w(z,\theta)$ can be calculated using either a concentration gradient or a vapour pressure gradient; the result will be the same in either case. If, however, a thermal gradient is present as in microwave drying, a relation such as (3.3.5) should be used.

A potential advantage in the use of microwave power would therefore appear to be its ability to produce large temperature gradients inside the material rather than outside. Figure 3.3.1 illustrates typical temperature profiles for both hot air drying and microwave-plus-air drying in a tray drier. The optimum situation, shown by curve 5, is one in which the relatively cool air is used only to carry away moisture. Because the highest obtainable temperature gradient is present, internal moisture movement should also occur at the highest possible rate. Drying air temperature must, however, be greater than the temperature at which the term $(p_o - p_w)$ begins decreasing with decreasing temperature faster than $\frac{dT}{dz}$ increases (equation (3.3.4)). With air at this minimum temperature, power density in the bed can be increased until the maximum vapour pressure is just below the mechanical stress limit of the wet material. If the vapour pressure is too high, diffusional losses will not drop the pressure to below one atmosphere before the surface is reached. Surface damage may occur as a result of liquid flashing to vapour in the relatively weaker surface layers. For the case of heat-sensitive materials, maximum temperature considerations will likely limit power density to well below the 'optimum' value for most rapid drying.

During diffusion-limited drying, a dynamic equilibrium will occur when heat input to the material is used entirely for evaporation:

$$\frac{dW}{d\theta} = \frac{A}{\bar{w}_s} G_w = - \frac{A}{\bar{w}_s} Y \left.\frac{dp_w}{dz}\right|_{z=0} \qquad \ldots (3.3.7)$$

If microwave energy is the only heat source,

$$\frac{dW}{d\theta} = \frac{3.41\, \bar{P}_d(\theta)}{\lambda_s} \qquad \ldots (3.3.8)$$

where $\bar{P}_d(\theta)$ = microwave power input to material near time θ (watts).

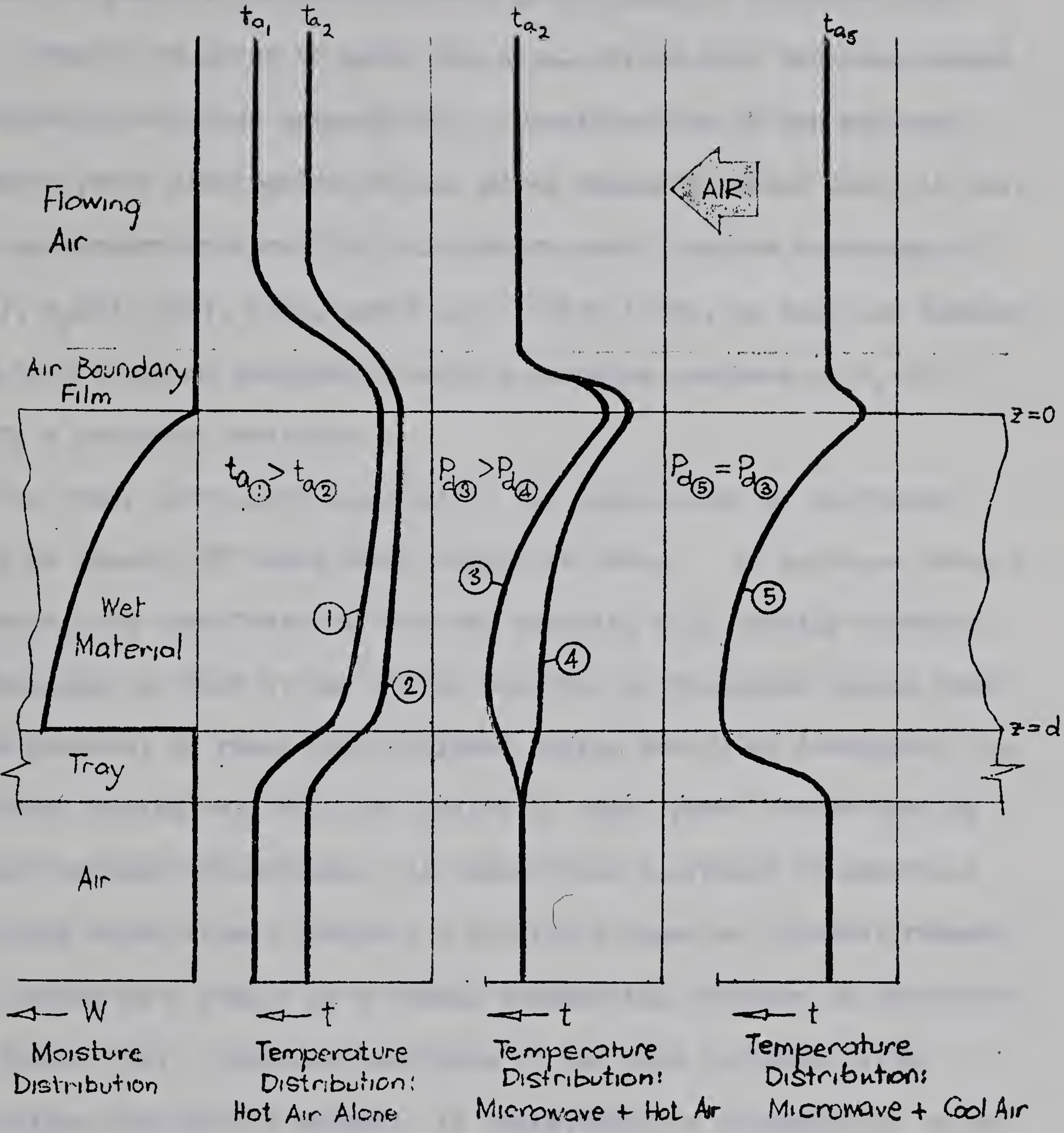
t_{a_1}
t_{a_2}
t_{a_2}
t_{a_5}
Flowing Air
AIR
Air Boundary Film
z=0
Wet Material
$t_{a①} > t_{a②}$
$P_{d③} > P_{d④}$
$P_{d⑤} = P_{d③}$
①
②
③
④
⑤
z=d
Tray
Air
← W
Moisture Distribution
← t
Temperature Distribution: Hot Air Alone
← t
Temperature Distribution: Microwave + Hot Air
← t
Temperature Distribution: Microwave + Cool Air

Figure 3.3.1. Typical Temperature Profiles for Diffusion Controlled Tray Drying.

Figure [illegible]

Implicit in the above is recognition of the fact that an equilibrium will not be possible unless microwave power input is decreased with time. This is required to match the usual drying rate decrease caused by decreasing moisture permeability. Determination of the maximum allowable power dissipation for any given vapour pressure limit is best made experimentally since its calculation would require knowledge of $W(z,\theta)$, $p_w(W)$, $Y(W)$, $W(\theta)$, and $T(z,\theta)$. With these, an equation similar to (3.3.4) could be integrated using a sorption isotherm at t_s to specify a boundary condition.

One other difficulty inherent in the application of microwave energy to removal of bound water should be noted. As moisture content decreases, the loss factor of the wet material will usually decrease substantially so that it may not be possible to dissipate enough power in the material to reach the 'optimum' drying rate just described. In this case, drying rate will be limited by input power rather than by moisture movement resistance. As temperature increases in materials containing bound water, however, a condition known as 'thermal runaway' often occurs as a result of a sudden exponential increase in dielectric loss factor [24]. Detailed knowledge of the loss variation with temperature for the wet material is consequently a prerequisite to the design of microwave driers for such materials. A very great improvement in diffusional drying rate should be expected with microwave power in any event for all materials with large diffusional resistances: for these, relatively little power will be necessary to produce a large vapour pressure gradient.

3.4 Capillary-flow Drying of Porous Materials

A brief phenomenological description of capillary-flow drying was

given in Section 2.2. It is generally accepted that capillary-flow controls drying in porous substances at moisture contents in excess of the hygroscopic limit (equilibrium moisture content). For hygroscopic materials, this limit is given as a function of relative humidity in a water sorption isotherm similar to that of Figure 2.2.1.

Analysis of capillary-flow drying has been approached both from scalar field theory, in analogy with diffusion [20], and from a strictly fluid flow standpoint [16]. The diffusion analogy uses an expression

$$G_w = - k_w \rho_s \frac{dW}{dz} \qquad \ldots (3.4.1)$$

where k_w = moisture 'conductivity' (ft.^{2}/hr.)

on which to base the analysis. Capillarity as such is not considered explicitly; its effects are lumped together in the parameter k_w which is treated in the same way as diffusivity. Unfortunately, k_w appears in practice to have a much stronger dependence than $\tilde{D}$ on such factors as moisture content, shrinkage, surface tension, viscosity, and temperature, so that application of equation (3.4.1) is limited to very simple problems in which k_w can be taken as a constant. Because of the sensitivity of k_w to material condition, even the problem of obtaining a reliable experimental relation for k_w may prove difficult.

A more fundamental analysis, due to Newitt [16,17], stems from the consideration of a porous bed of non-porous spherical particles under the action of a potential Γ:

$$\Gamma = \frac{X \sigma_T}{r \rho_w g} \qquad \ldots (3.4.2)$$

where: Γ = capillary 'suction' potential (ft. of liquid)

X = a packing factor (dimensionless)

σ_T = liquid surface tension (lb./sec.^{2})

r = effective particle radius (ft.)

ρ_w = density of water (lb./ft.^{3})

g = acceleration of gravity (ft./sec.^{2}).

Except for use of a packing factor and particle radius rather than capillary radius r_c, this expression is identical to the classical capillary rise equation for small capillaries:

$$\ell = \frac{2\,\sigma_T}{r_c \rho_w g} \qquad \ldots (3.4.3)$$

The suction potential, in effect a head differential, must overcome both static head d, if the water is drawn effectively from the bottom of the bed, and frictional resistance h_L to the flow G_w. Newitt's expression, a modified Poiseuille equation for laminar flow, gives:

$$h_L = \frac{\bar{\mu} V_f \rho_s^2\, S^2 (1 - F_1)^2 d}{g \rho_w F_1^3} \times 10^6 \qquad \ldots (3.4.4)$$

where: h_L = head loss over a distance d (ft. water)

$\bar{\mu}$ = dynamic viscosity of water (lb./ft.sec.)

V_f = moisture flow velocity (ft./sec.)

ρ_s = particle absolute density (lb./ft.^{3})

S = specific surface of particles (ft.^{2})

F_1 = bed porosity (dimensionless)

d = bed depth (ft.)

Since water is being drawn from larger pores, the effective head differential $(\Gamma)_{eff}$ is the difference between Γ_1 at the surface in small pores and Γ_2 at the mean water level in the large pores. Evidently, $(\Gamma)_{eff}$ is a function of moisture content: it will be zero for $W = W_c$, increase as the larger pores empty, and finally decrease again to zero as water is drawn from pores of increasingly small diameter.

Assuming rhombohedral packing of particles, Newitt obtained:

$$\left(\frac{dw}{d\theta}\right)_{fc} = \frac{16.1\ yr^2}{d}(\Gamma_1 - \Gamma_2 - d) \qquad \ldots (3.4.5)$$

where: $\left(\frac{dw}{d\theta}\right)_{fc}$ = drying rate during capillary-flow limitations (lb./ft.^{2}sec.)

y = fraction of fine pores at surface

r = particle radius (ft.)

Γ_1 = surface value of suction potential (ft. water)

Γ_2 = mean internal suction potential

d = bed depth (ft.).

Good agreement between calculated and experimental drying rates was reported for silica flour and glass spheres using measured values of Γ_1, Γ_2 and y.

Again, it is evident that the use of microwave power may increase the drying rate substantially. Three areas of potential improvement are available. The first is simply an extension of the improvement to constant rate drying since the bulk of evaporation occurs at the bed surface in the menisci of fine capillaries. Gross drying rate decreases only because evaporating surface area is decreasing as larger capillary water surfaces recede into the bed. Another expected increase over conventional drying rate will be caused by increased evaporation rate at internal liquid surfaces. The resulting vapour will flow to the bed surface in response to the vapour pressure gradient. Decreasing the air stream temperature, since the air is no longer the primary heat source for drying, will further increase the drying rate by increasing the vapour pressure differential. Internal drying in substances with a large proportion of fine pores will be limited by vapour-phase flow resistance at high drying rates so that any increase in pressure

gradient will tend to increase drying rate. The third rate-increasing effect of microwave power will be to increase the suction potential $(\Gamma)_{eff}$ through a decrease in Γ_1 caused by higher internal vapour pressures. This last effect should be negligible for most of capillary-flow drying since suction potentials should be orders of magnitude greater than the forces $\pi r_c^2 \Delta p$ for all but the largest capillaries.

An estimate of the magnitude of capillary-flow drying rate increase can be obtained by considering the first two effects separately. Drying at the surface will increase by a percentage Δ_1 at any time θ where:

$$\Delta_1 = \left\{ \left[y\, e^{-2\alpha_d d'} \right] \frac{3.41\ \bar{P}_d(\theta)/\lambda_s}{\left(\frac{dw}{d\theta}\right)_a} - 1 \right\} \times 100\% \qquad \ldots (3.4.6)$$

where: $\bar{P}_d(\theta)$ = microwave power absorbed over the evaporating surface (watts/ft.^{2})

λ_s = latent heat of vapourization of water at temperature t_s (BTU/lb.)

$\left(\frac{dw}{d\theta}\right)_a$ = drying rate for air alone (lb./hr.)

$d' = d\left[\frac{W_{c1} - W(\theta)}{W_{c1} - W_{c2}}\right]$ = mean depth of internal evaporation (ft.)

W_{c1} = critical moisture content (start of falling rate period)

W_{c2} = moisture content at the end of capillary-flow limited drying.

Because of the relatively low internal vapour pressure gradients associated with hot air drying, almost all evaporation will occur at the material surface. Thus, $\left(\frac{dw}{d\theta}\right)_a$ is the total hot air drying rate. In the microwave drying case, however, appreciable energy may be used for internal evaporation so that the factor $y \exp\{-2\alpha_d d'\}$ has been included to compensate for this.

Movement of water vapour through open pores can be described by an expression for the flow of a compressible fluid through a bed of granular material [17]:

$$G_v = \left\{ \frac{gM_w\,(p_M^2 - p_{ws}^2)}{2\tilde{Z}RT} \left[\ln\left(\frac{v_M}{v_s}\right) + F_2 \right] \right\}^{\frac{1}{2}} \qquad \ldots (3.4.7)$$

where: p_M = maximum absolute vapour pressure (psia)

p_{ws} = surface absolute vapour pressure

g = 32.17 lb.mass-ft./lb.force-sec.^{2}

M_w = vapour molecular weight (lb./lb.mole)

$\tilde{Z}$ = vapour compressibility factor (dimensionless)

R = gas constant = 1546 ft.-lb.force/lb.mole-°R

v_M = vapour specific volume at p_M (ft.^{3}/lb.mass)

v_s = vapour specific volume at p_{ws}

F_2 = a bed structural factor depending on particle shape, particle diameter, a friction factor, bed depth and bed porosity.

The reader is referred to Perry, section 5-50, for the complete expression and for details of the factor F_2.

To determine the effect of increasing bed internal temperatures, the ratio of vapour mass flow rates at two temperatures T_1 and T_2 can be calculated using a Clausius-Clapeyron relation to express the vapour pressures in equation (3.4.7) as a function of T:

$$\frac{G_{v2}}{G_{v1}} \simeq \left[\frac{T_1}{T_2}\right] \frac{e^{-2/T_2} - e^{-2/T_s}}{e^{-2/T_1} - e^{-2/T_s}} \qquad \ldots (3.4.8)$$

Variations in the term $\ln\left(\frac{v_M}{v_s}\right)$ have been neglected. For T_1 = 340°K, T_2 = 370°K, and surface temperature T_s = 300°K for both cases, the ratio

is only 1.47. Since drying by internal vapour movement is itself a secondary effect, use of microwave power will not, contrary to expectations, produce any real drying rate advantage through increased internal vapour movement. Drying rate improvement will thus be confined, for porous materials, to the increase in external surface evaporation rate during capillary-flow limited drying.

In non-porous materials, internal vapour movement will occur by a diffusion mechanism and as such will be indistinguishable from liquid diffusion. Differences between liquids and gases disappear when flow is being considered on a molecular scale as in diffusion. Gas diffusivity is normally a function of $T^{3/2}$ so that the ratio of mass diffusion rates for air and for microwave-plus-air drying is, approximately:

$$\frac{G_{vma}}{G_{va}} \simeq \left[\frac{T_{ma}}{T_a}\right]^{\frac{1}{2}} \left.\frac{\left(\frac{dp_w}{dz}\right)_{ma}}{\left(\frac{dp_w}{dz}\right)_a}\right|_{z=0} \qquad \ldots (3.4.9)$$

The importance of surface temperature and of vapour pressure gradient in determining the drying rate is apparent here. The use of microwave power may therefore be expected to give substantially increased vapour diffusion rates in such materials.

Unfortunately, even these rather involved expressions are inadequate to describe moisture movement in the complex materials encountered in the bulk of drying problems. Liquid diffusion and capillary flow often work together so that separation of their respective effects is all but impossible. The preceding discussion will serve, however, to outline the general character of processes involved, to indicate some of the primary variables with their basic inter-relations, and to point out the areas of potential advantage in the use of microwave power.

3.5 Practical System Evaluation

One point will be very clear by this time: drying, despite over a half century of intensive investigation, is still an empirical technology. Now and then, a particularly illuminating theory such as Brunauer's work [26] on adsorption phenomena provides a deeper insight into drying mechanisms, but, in general, the complexity of the physical situation defies the development of a truly basic analysis which can be used with confidence for design. In the preceding three subsections, the drying relations presented invariably include a parameter which, although supposedly a constant of the system, is in fact dependent on one or more of the drying variables. Evaluation of the parameter for an actual drying problem, except for relatively simple cases, must rely on experimental data from a system very similar physically to the system being analyzed and with wet material identical to that which is to be dried in practice. For details of conventional drier evaluation procedures, reference should be made to such recent publications on dehydration and drying as Van Arsdel [20] and Perry [17]. Only those aspects directly related to a microwave evaluation will be presented here.

A typical problem in connection with microwave drying will involve:

i) choice of a microwave system or applicator configuration

ii) specification of the best frequency and power level range for the drier

iii) estimation of system efficiency

iv) specification of a suitable pilot system to be used to obtain actual drying data

v) specification of suitable conditions under which to conduct drying tests

vi) estimation of allowable power input as a function of moisture content under specified vapour pressure or temperature limitations

vii) estimation of the material time-temperature relation expected for the drying of materials which exhibit some degree of temperature sensitivity.

Because of the wide range of possible systems and materials, the following discussion will be of a general nature.

The choice of drier type is usually the first step in system specification. Depending on the process from which the wet feed is being drawn, the drying stage may be required to be either a continuous or batch operation. In some situations, there will be no such restrictions placed on the product flowrate. Feed material characteristics and desired product qualities can be used to eliminate unsuitable drier types from further consideration. For example, the drying of a powder suspension, done conventionally with twin-drum, pan or spray driers, would likely be best approached from a microwave standpoint with a pneumatic conveying or a spray system. Paper on the other hand, because of its relatively high loss factor even when dry, must be moved quite rapidly through the drier to avoid damaging heat build-up. The short residence time will necessitate many passes through the drier, or a multi-stage drier, with cooling between stages. A waveguide, slotted longitudinally and run in a continuous series of wide parallel meanders, is an inexpensive but effective applicator. In most cases, a suitable configuration will be apparent from similar considerations.

Having settled tentatively upon an applicator, system frequency should be chosen. The choice will usually be a compromise between depth of penetration (equation 3.1.8) and dissipated power density (equation 3.1.1) requirements. Higher frequencies will allow higher dissipated power

densities but will also decrease the depth of the layer in which the power is absorbed. In an extreme case, the microwave power will be dissipated almost entirely near the surface which will produce, under falling-rate conditions, surface overheating and a drying rate no higher than the equivalent hot air system. Use of lower frequencies should give the penetration essential to effective use of the microwave energy, but higher field strengths will be required to maintain power dissipation and conductor losses in guiding structures will increase. Mismatch at the dielectric surface will also increase with decreasing frequency, resulting in less power being transmitted into the substance and more power reflected toward the generator. The amount reflected will materially affect generator stability and life. For systems with large power requirements, the frequency should be chosen as high as possible by use of minimum practical bed depth. Available high power microwave generators are limited at present to the two ISM frequencies of 915 MHz and 2450 MHz. Bed depth should be adjusted if possible to equal the penetration depth at the higher of these frequencies.

Some knowledge of the dielectric and drying characteristics of the material are necessary to proceed with power specifications. A material which dries by diffusion will require a wide variation in power input over the drying time, ranging from a maximum set by vapour pressure or temperature limits to nearly zero for a well-insulated system near the material equilibrium moisture content. A bed of non-porous large granules, however, can be dried using substantial amounts of power during all phases. To obtain maximum expected power input to the material, equations (3.2.15) and (3.2.18) can be solved to obtain t_s and $t_M - t_s$ for a given power dissipation $\bar{P}_d$. For some $\bar{P}_d$, t_M will equal either a temperature limit specified for the particular material or, in the absence of such

a limit, a temperature slightly below the boiling point of water. This establishes maximum allowable power dissipation.

Conventional driers require between 1200 and 6000 input BTU per lb. of water evaporated depending upon design. A pound of water will require at least 1000 BTU for its vapourization giving corresponding thermal efficiencies of from 83% down to only 7%. Because of the cost of microwave energy, every effort will have to be made to minimize losses. The drier should be well-insulated and heat exchange equipment used to recover heat from product discharge, exhaust air, microwave generator and wave-trap systems. Due to the internal heating characteristic of microwave energy, a microwave system can be reasonably expected to have an efficiency based on input h-f power in the region of 80 to 90%.

Knowing the applicator type, system frequency and power level, a designer may then develop a suitable pilot drier with which to obtain detailed drying information. The test unit should be large enough to allow bed depth to equal the anticipated full-scale depth unless it is possible to scale down penetration depth effects by a frequency increase. Since tests will be done with power levels of between 1 and 25 kw (about 3 to 75 lbs. of water per hour at 1200 BTU/lb. of water evaporated), generators for the higher frequency may not be available. Drier loading will vary with the material: only small quantitites of a material which dries very quickly can be handled at optimum drying rates, while slowly drying materials can be tested in larger quantities before the effects of input power limiting appear.

Air velocities in excess of 400 ft. per minute are recommended in keeping with normal drying practice, with a maximum of about 1200 ft. per minute. These figures are useful for static beds of materials only;

through-circulation or fluidized-bed requirements will be very different. Inlet air humidity H_1 should be below 10 percent and the difference $(0.4H_{02} - H_1)$ sufficient to accept the moisture input at the highest required drying rate (H_{02} = saturation humidity at drier outlet temperature). Inlet air temperature will be dictated by whether or not auxiliary hot air drying is desired and by material temperature sensitivity. For microwave drying without hot air assist, air temperature should be kept as low as possible consistent with an outlet relative humidity of 40 percent or less. Other conditions which must be specified will depend on the specific drier type being tested.

Drying data, usually obtained under conditions of constant air temperature and humidity, are basically a moisture content-time relationship. Material temperature and exhaust air temperature and humidity are generally measured in addition. Typical W vs. θ curves are given in Section 4. To display drying periods more clearly, the drying curve is differentiated graphically and the drying rate plotted against moisture content. From this curve, the critical moisture content can be taken and falling-rate mechanisms postulated. The falling-rate drying phases are best analysed using a graph of $\ln(W - W_e)$ vs. drying time. In simple systems, diffusion-controlled drying will produce a straight-line relationship on such a plot. With this information, and for hygroscopic materials, an equilibrium moisture content vs. relative humidity curve, the relations presented in Section 3 can be used to evaluate drying characteristics under other conditions. It should be emphasized that drying is highly dependent on material history and such predictions should be used with caution.

Once estimates of $W(z, \theta)$ and $t\ (z, \theta)$ are available, a more detailed analysis of the system from a microwave standpoint is possible if $\varepsilon(t, W)$ is known or has been measured. Mismatch at the bed surface and reflection

magnitudes and mode patterns can also be calculated to allow positioning of the material in the best relation to expected fields. The change in tuning of a resonant system as drying progresses can also be estimated, and if necessary, provision made to retune automatically on the full-scale system. Feed and discharge slots should be kept as small as possible, certainly well below the dimensions of the system air wavelength, to minimize both unnecessary power radiation losses and hazard to operating personnel. In some cases, field attenuating structures will be necessary at enclosure openings to keep external fields within a safe value. These should be designed with the recovery of absorbed energy in mind. Material conveying or containing devices which are inside the microwave system must be constructed from such low-dielectric loss materials as teflon, polypropylene, polystyrene and pyrex; in general, any substance free from polar constituents and of low electrical conductivity will be suitable for this purpose.

Several of the preceding points will be discussed in later sections in connection with an economic evaluation of microwave drying. To illustrate the physical behavior of microwave drying systems, some results obtained in a laboratory drier will be presented in the next section.

4.0 DRYING BEHAVIOR IN AN EXPERIMENTAL SYSTEM

4.1 Description of the Drier

In keeping with the general nature of this investigation, experimental work was confined to obtaining a qualitative picture of the behavior of various wet materials in relatively high power microwave fields. The drying system used was consequently a very simple one involving a rectangular 74.4 litre multimode resonant cavity loop-coupled to a 2450 MHz, 1 KW (nominal) CW magnetron source (Figure 4.1.1). Air was supplied and exhausted through circular wave-guides beyond cutoff which were attached to the cavity roof. A hot-air gun controlled by a variable transformer was used as an air source. No provision was made to retune the cavity as moisture content changed; rather, dissipated power in the wet material has been considered equal to measured dissipated power in an equivalent volume of water. Since coupling to a reasonably lossy dielectric load in a resonant cavity depends only on the volume to surface area ratio of the load for a given frequency (to a rough approximation, see Voss [23]) this was considered a valid procedure. The measured variation of $\bar{P}_d$ with volume for a water load is illustrated in Figure 4.1.2.

The material was held in a pyrex tray set on four pyrex supports. Because this physical arrangement could be expected to result in a somewhat complex air flow pattern, it was decided to measure the effective flowrate over the tray surface rather than use some approximate function of the input air flowrate. This was accomplished by filling the tray with water and measuring the evaporation rate $dw/d\theta$ for various air gun voltages between 35 and 100 volts with heater off. If the wet- and dry-bulb temperatures t_w and t_a are also measured, the effective mass flowrate

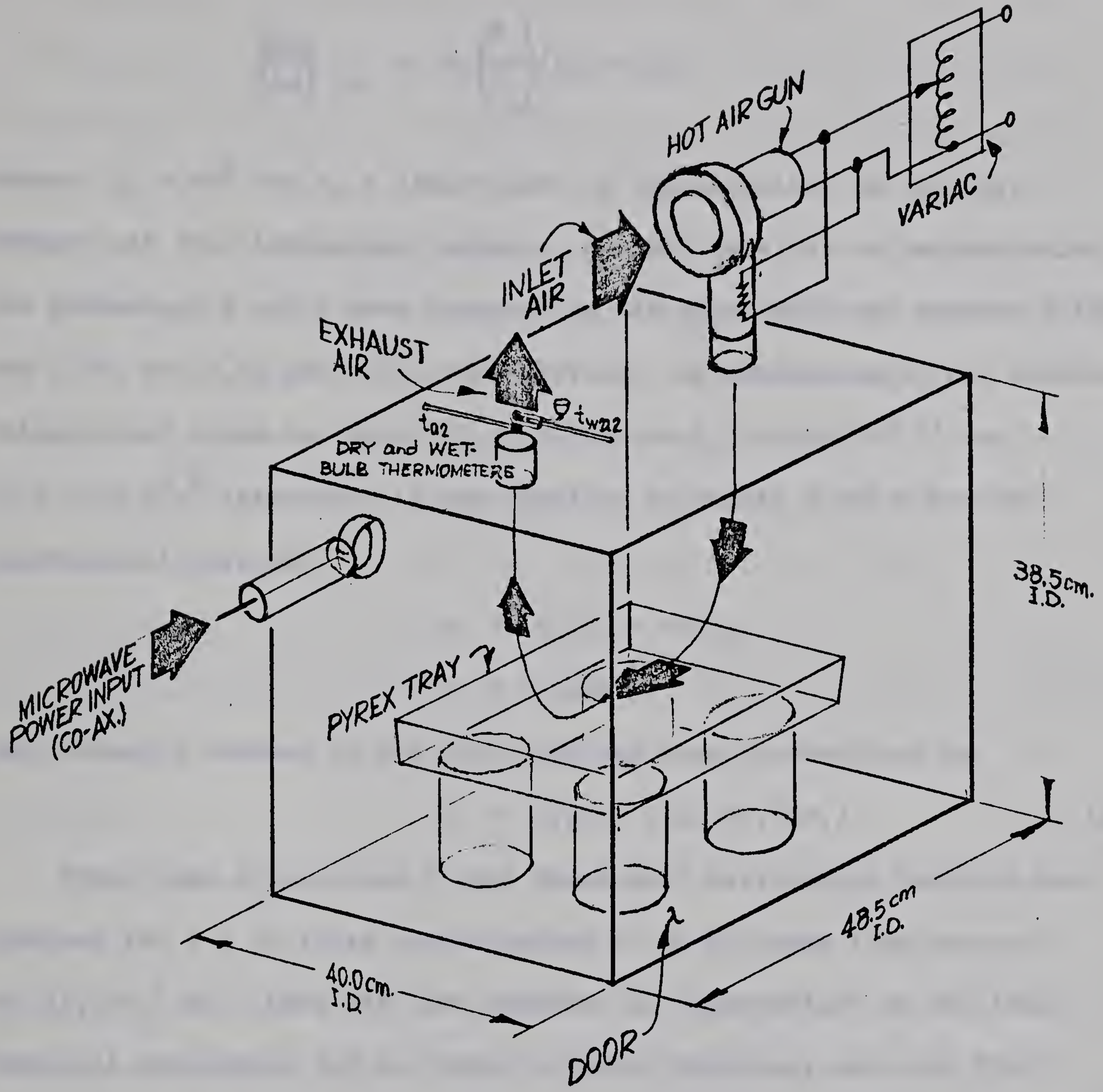
HOT AIR GUN
VARIAC
INLET AIR
EXHAUST AIR
ta2
twa2
DRY and WET-BULB THERMOMETERS
MICROWAVE POWER INPUT (CO-AX.)
PYREX TRAY
38.5 cm. I.D.
48.5 cm I.D.
40.0 cm. I.D.
DOOR

Figure 4.1.1. The Experimental Drying System

G over the water surface can be calculated from h_c using (3.2.7):

$$\left(\frac{dw}{d\theta}\right)_{cc} = h_c\left(\frac{A}{\lambda_s}\right)(t_a - t_s)$$

where: $h_c = aG^n$ and λ_s = latent heat of vapourization at $t_w = t_s$. Because air flow impingement appeared as much parallel as perpendicular, the parameters a and n were expected to lie about half way between 0.128 and 0.37, and 0.37 and 0.80, respectively. By evaluating h_c for various voltages and using the point (h_{co}, G_o) where $h_c = 0.128\ G^{0.37}$ and $h_c = 0.37\ G^{0.8}$ intersect, it was possible to obtain a and n for the experimental case as:

$$n = 0.575 \pm 0.011$$

$$a = 0.198$$

Fan voltage V between 35 and 100 volts was then related to G by

$$G = 9.26\ V\ (\text{lb./ft.}^2\text{hr.}) \qquad \ldots\ (4.1.1)$$

After some trial runs, it was found that best drying behavior was obtained for V = 70 volts corresponding to an air mass flow rate of 650 lb./ft.^2 hr. Less air flow resulted in 'sputtering' in the fine materials apparently due to vapour pressure build-up; more air flow disturbed the water film appreciably which would result in the drying surface being some unpredictable amount more than the tray cross-sectional area.

Material temperature measurements were done with power off just before weighings. Exhaust air dry- and wet-bulb temperatures were monitored in the exhaust waveguide using carbon tetrachloride-filled glass thermometers. Material temperatures were measured with a thermocouple and VTVM for fast response. Temperature measurements are considered accurate to within 2°C.

Tray weighings were done on a 10 kg. single beam balance. It was possible to obtain readings reproducible to within 0.5 gm. Some difficulty was encountered near the critical moisture content where evaporation continued at an appreciable rate during weighing. It was found that this effect was negligible if the weighing was done within 15 seconds of removal from the drier.

Although some 30 to 37 modes have been identified in this cavity [9], the power density was not as uniform as might be expected. At least four small regions within the cavity contained particularly high field intensities. These regions, generally known as 'hotspots', occurred symmetrically at the tray height about 9 cm. from front and rear walls and 8 cm. from side walls, and were about 3 cm. in diameter. The carmelization of portions of a tray of cornstarch served to delineate the hotspots. Several others of a relatively minor nature were also apparent.

For several tests, it became necessary to reduce the power being absorbed by the wet material in order to avoid sputtering (vapour eruptions) or overheating. The generator was not equipped with a power controlling circuit so that an auxiliary water load was added to the cavity when necessary to absorb excess power. The weight of water in the auxiliary load was usually increased according to the decrease in material water content. Evaporation losses were also made up at each weighing. In several cases, when an auxiliary load was required, the wet material and water load were placed in two identical trays of inside dimensions 15.75 cm. x 25.0 cm. x 4.75 cm. and set in the cavity so that air passed over the material tray first.

In order to estimate the division of power between two such trays, power absorption in water loads was again measured, giving rise to the distribution shown in Figure 4.1.3. The rather odd characteristic

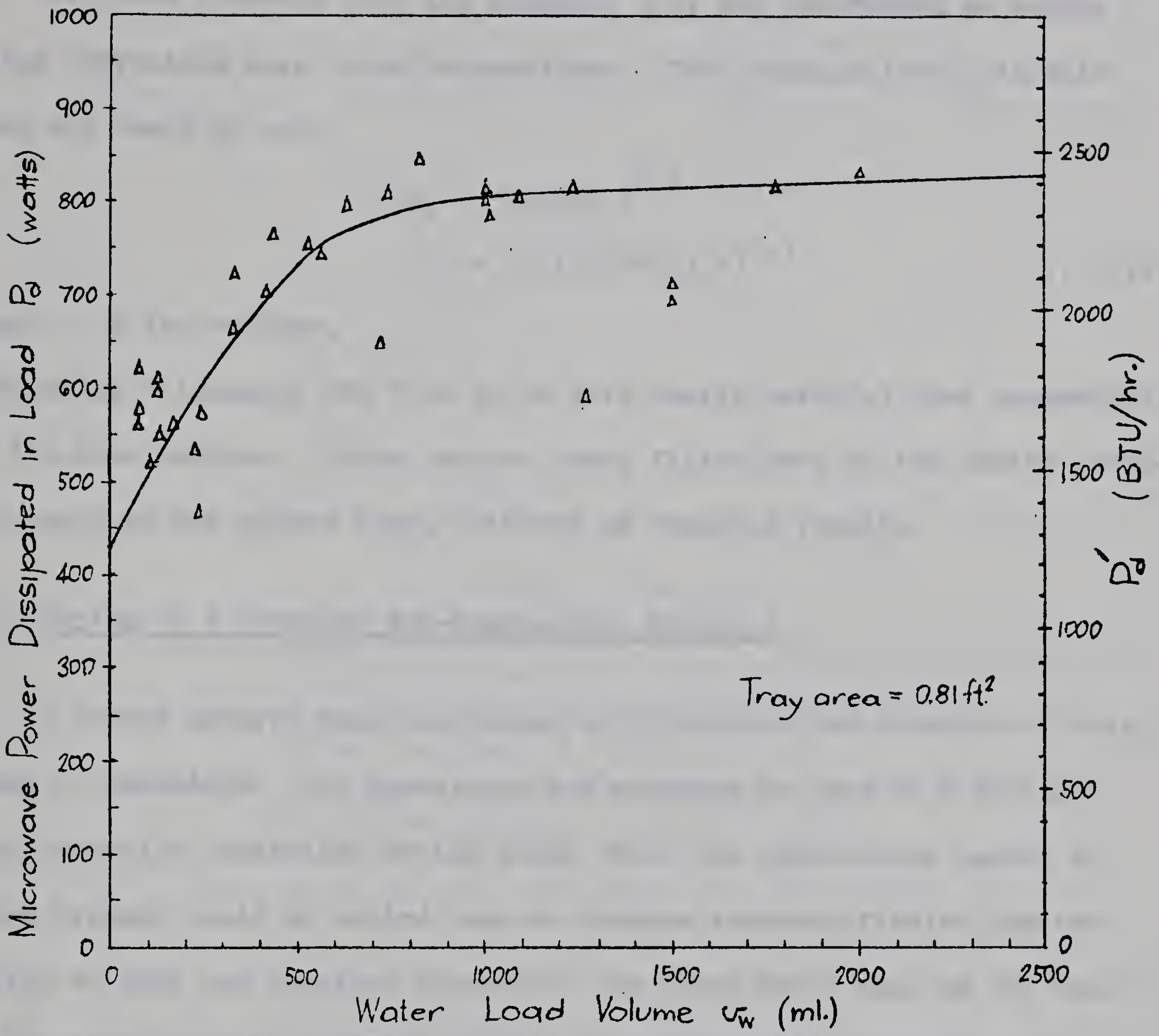

Figure 4.1.2. Variation of Power Absorbed by a Water Load

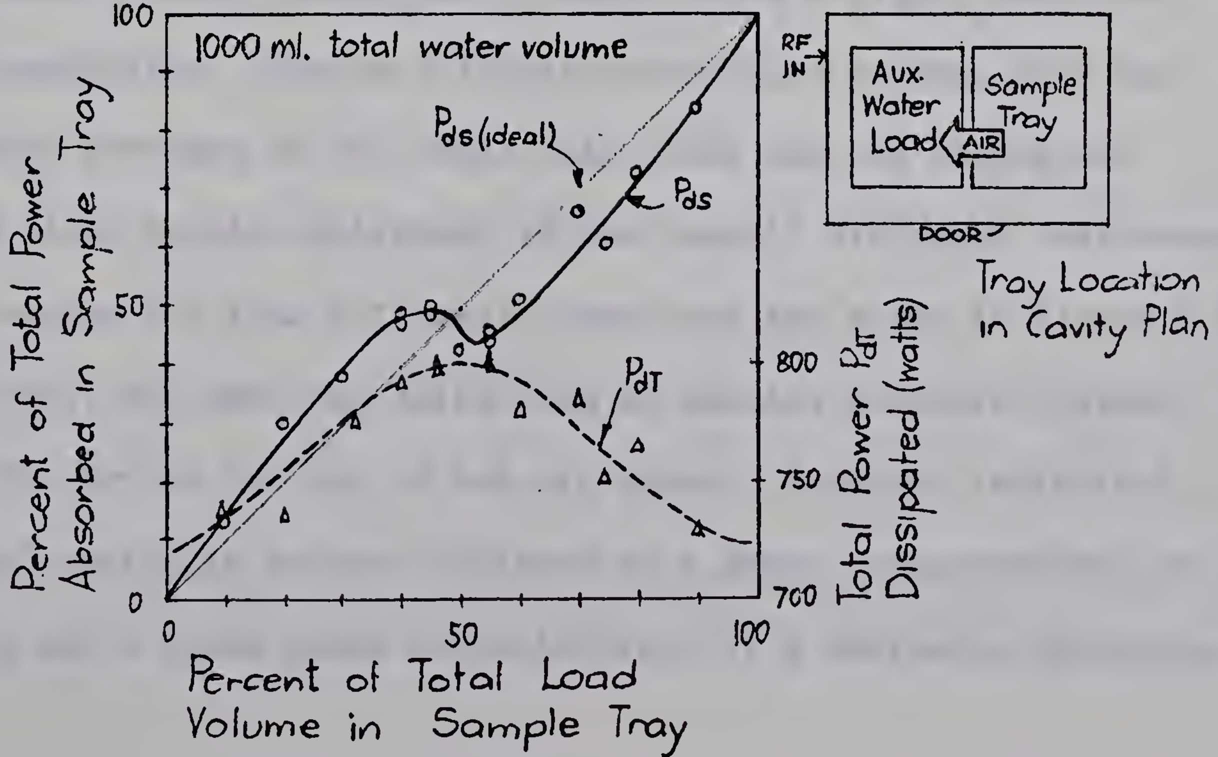

Figure 4.1.3 Division of Power between Two Water Loads

obtained is believed a result of a major mode distribution change as water load balance shifts from one side to the other.

Air mass flowrate over the material tray was determined as before using convective mass transfer equations. The relation for h_c in this case was found to be:

$$h_c = 0.163\, G^{0.7}$$
$$= 0.163\, (4.57\, V)^{0.7} \qquad \ldots (4.1.2)$$

where V = fan voltage,

indicating a tendency for flow to be more nearly parallel than perpendicular to the tray surface. Since the two trays filled more of the cavity cross-section than the single tray, this was an expected result.

4.2 Drying of a Granular Non-Hygroscopic Material

A coarse natural sand was chosen to illustrate the behavior of this class of materials. The coarseness was expected to lead to a definite capillary-flow controlled drying phase while the appreciable amount of fines present could be relied upon to produce vapour-diffusion limited drying at very low moisture contents. The clays which made up the bulk of the fine material normally exhibit some hydrophilic tendency, but because they were a minor constituent, their effect a higher moisture contents was negligible. During diffusion-controlled drying, both the decreased vapour pressure in the small clay pores and the adsorptive nature of the clays should contribute to the overall diffusion resistance.

Drying results for four different situations are given in Figure 4.2.1. In the first case, the sand was dried from an initial moisture content of 0.217 lb./lb. dry by the use of hot air alone. A rather indistinct "constant-rate" period is evident followed by a phase characteristic of capillary-flow and a final phase characteristic of a diffusion mechanism.

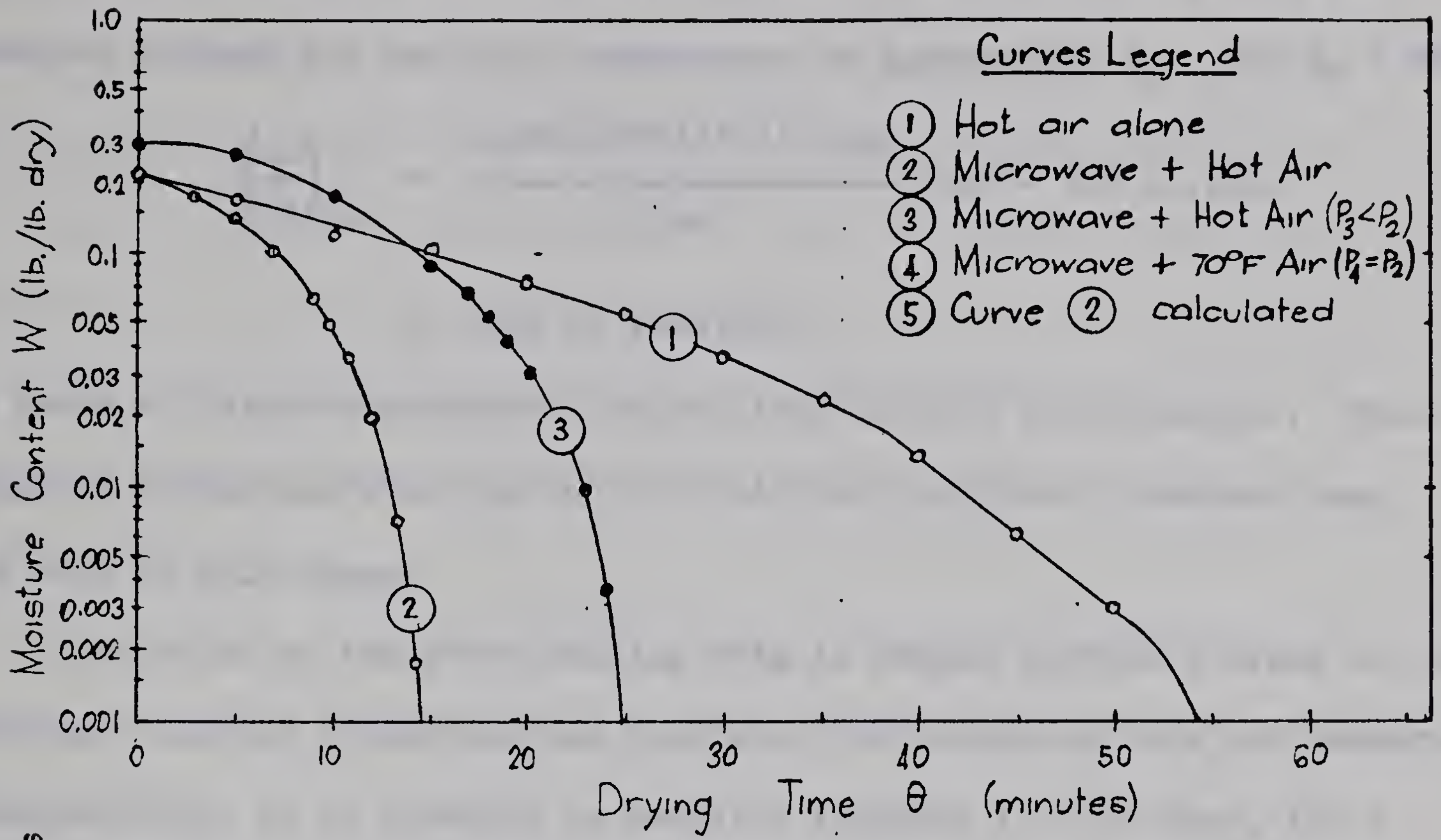

Drier Conditions

Microwave: cavity vol. = 74.4 l. (2.62 ft^3); nominal generator power = 1 kw; approx. power into mat'l: $P_1=0$; $P_2 = 805$ w. (max.); $P_3 \cong 600$ w. (max.)

Inlet Air: temp. $t_a = 230°F$; humidity $H_a = 0.008$ lb./lb. dry; mass flowrate $G = 785$ lb./ft.^{2} hr.

Material: dry weight $w_S = 3.02$ lb.; tray area $A = 0.81$ ft^2; sand bulk density $\rho_s' = 93.6$ lb./ft^3.

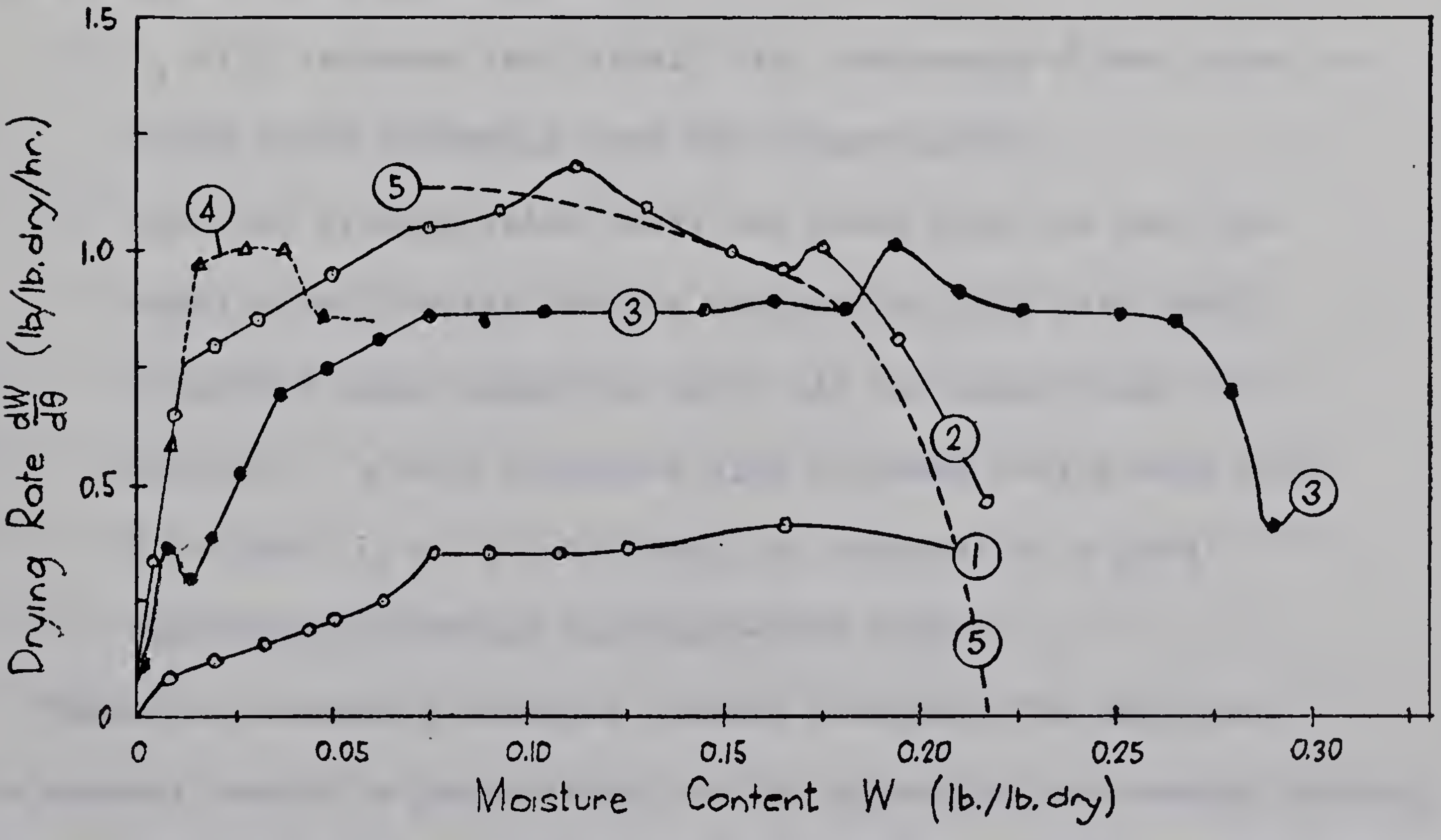

Figure 4.2.1. Drying of a Coorse Natural Sand (90% + 150 mesh Tyler) in a Microwave Tray Drier at 2450 MHz.

Critical points are at 0.073 and 0.014 lb./lb.dry. Referring to equation (3.2.7), the expected constant drying rate can be calculated using the measured exhaust air wet-bulb temperature to approximate t_s. For t_w = 86°F,

$$\left(\frac{dw}{d\theta}\right)_{cc} = \frac{0.198\ (785)^{0.575}\ 0.81}{1044}\ (230 - 86)\ \text{lb./hr.}$$

$$= 1.02\ \text{lb.water/hr.}$$

In terms of relative moisture content, this is 0.34 lb./lb.dry-hr. This compares favourably with the 0.35 to 0.40 lb./lb.dry-hr. measured over the bulk of this phase.

Prediction of the first falling rate is rather difficult owing to the fact that suction potentials and pore size distributions were not measured. Qualitatively, it is observed in Newitt's relation (3.4.5) that, for a given system, drying rate depends on $(\Gamma_1 - \Gamma_2)$, y and r^2, each of which may vary to some extent with moisture content. The potential difference, however, should not change appreciably over most of the capillary flow drying period. This arises from:

i) Γ_1 will increase very slowly with decreasing W when water is being drawn primarily from the larger pores.

ii) once the average water level has moved into the bed, the capillaries feeding surface evaporation will have radii of nearly equal magnitude until all the large pores are emptied. Γ_2 will therefore also increase very slowly with W so that $(\Gamma_1 - \Gamma_2 - d)$ should be constant to a good approximation during capillary-flow drying.

Since the remaining moisture content available for capillary flow removal should be proportional to the square of the average flowing capillary size, and consequently to the particle radius r involved with

the flow, it is possible to use, if y is constant:

$$\overset{\circ}{w} = K_1 W$$

where K_1 is a constant. However, as drying proceeds, the area Ay of the capillaries feeding the surface will decrease, rapidly at first as the larger pore menisci containing most of the evaporating area recede into the bed, then more slowly as the levels in the smaller capillaries drop. The overall effect should be a drying characteristic with positive curvature during capillary-flow drying. Experimentally, it was found that:

$$\overset{\circ}{w} \simeq K_2 W^{2.5} + K_3 \quad (K_2 \text{ and } K_3 \text{ constants})$$

provided a good fit to the data. If the preceding explanation is valid, we must have:

$$y \propto W^{3/2}$$

Because the fractional area y will depend on r^2 for a given pore size, the above relation implies a particle size distribution at the surface of:

$$n_r \propto r$$

where n_r = number of particles with radius r. An explanation for such a distribution is not readily apparent.

In any case, a short diffusional-flow final phase occurred as expected. The second critical point W_{c2}, coinciding with the observed complete drying of the bed surface, appeared at extremely low moisture contents because of the gravity separation of fines and coarse material in the bed. Drying surface area should decrease very slowly in the first falling rate period if most of the fine material is at the top of the bed. Coarse material below would assure an adequate water supply for the surface capillary layer until the bulk of the remaining moisture resided on the coarse particle surfaces and in the surface layer. At

this point, very restricted vapour flow would begin and characterize the final drying phase.

On the basis of this explanation of air drying behavior, the microwave drying may be examined. In one case, input power was allowed to vary with cavity loading as given in Figure 4.1.2; in the other, a water load was added to drop power input to the material for comparison purposes. Water was added as necessary to maintain total cavity 'wet volume' (volume occupied by water or by wet material) constant. The concept of wet volume will be valid even at very low moisture contents in a resonant system so long as the necessary volume filling factor, in this case at least 1.5% of cavity volume, is exceeded [23]. For the 1372 gm. sand bed, bulk volume was 915 ml. with a porosity of 0.246; thus wet volume v_w is:

$$v_w = \begin{cases} 690 + 1372W \text{ for } W > \dfrac{225}{1372} = 0.164 \\ 915 \text{ for } W_{c2} < W < 0.164 \\ 915\left(\dfrac{W}{W_{c2}}\right) \text{for } W < W_{c2} \end{cases}$$

where all volumes are in ml.

With no auxiliary water load, drying rate rose until all input power was being used for evaporation (curve 2, experimental; curve 5, calculated for similar conditions). By means of equation (3.2.18), the following conditions were calculated for the maximum drying rate (wet volume = 915 ml.):

$\bar{P}'_d$ = 2740 BTU/hr. (Figure 4.1.2)

H_s = 0.136 lb./lb.dry

t_s = 137.5°F

c_s = 0.30 BTU/lb.°F

λ_s = 1016 BTU/lb.

p_{ws} = 0.17 atm.

The predicted drying rate with these values is 1.10 lb./lb.dry-hr. compared to 1.18 observed. Continuation of drying by natural convection during weighings should account for most of the discrepancy. Below this moisture content, drying entered an early falling-rate period, characteristic of capillary-flow limiting, rather than the constant-rate period expected. It was not possible to correlate this drop with either microwave power input decrease, which should have been comparatively small, or high drying rate existing, since other drying tests exhibited the early drop-off at a lower rate than was observed for "normal" behavior. Only one feature of the drying appeared to be present each time an "early" falling-rate period occurred: this was a relatively rapid change in drying rate. The early critical point did not appear after a fairly long period of truly constant rate drying. Optimum drying time will thus involve insuring that, as bed saturation moisture content is neared, the drying rate is made very nearly constant.

The reason for such behavior may be the following. When surface moisture has been evaporated and bed saturation is reached, moisture begins to be drawn from within the bed as previously described. Uniform moisture movement will tend to help maintain this progressively more unstable situation until the critical moisture content is reached. At about W_{c1}, the bed surface begins to decrease abruptly resulting from the breaking of the surface moisture layer. Rapidly changing evaporation, on the other hand, will be more likely to cause the surface moisture layer to break up early because surface layer moisture gradients will not have had time to equalize before the layer breaks.

In each test, a very definite critical moisture content is reached which is almost independent of drying rate. The subsequent falling-rate period for microwave drying has a linear variation with W suggesting, on

the basis of behavior postulated for air drying, that dependence on decreasing external surface evaporating area may have been removed. Area dependence of drying rate would be apparent if the average slope of the rate curve increased with rate: the higher the drying rate, the fewer capillaries that will be able to maintain flow to the surface. While a small difference in slope is noticeable between curves 1 and 2, the microwave curves have identical slopes despite a large difference in drying rates. For a capillary-flow mechanism, this implies that evaporation must be occurring at internal water surfaces almost as rapidly as at the external surfaces. Such a situation is quite conceivable for a porous material, having only a minor vapour flow resistance, drying under a positive internal vapour pressure gradient. A positive dp/dz will not be found in hot air tray drying unless heating is done through the tray bottom. The sand bed was also dried with ambient temperature air over the low moisture content range. A substantial increase in capillary-flow drying rate was observed, confirming the prediction of Section 3.4 that such an increase should result from increased vapour pressure gradients.

The final drying phase beginning at $W_{c2} = 0.014$ lb./lb.dry, the same moisture content as for air alone, indicates that vapour diffusion may be the limiting mechanism in the microwave drying also. A nearly linear variation is quite obvious which is characteristic of the late stages of diffusion. The sand bed was heating rapidly at this time so that power limiting was not suspect. If equation (3.3.2) is differentiated with respect to time, one obtains, for large θ, the simplification:

$$\mathring{W} = \frac{dW}{d\theta} = -a\,(W - W_e) = -\frac{\pi^2 \tilde{D}}{4d^2}\,(W - W_e)$$

While θ is definitely not large in this case, it appears that the presence of microwave fields may yield a similar type of vapour pressure gradient to that for θ large. This implies that vapour pressure gradient is proportional to moisture content, an equilibrium condition which would exist for air drying only after diffusion had adjusted and stabilized moisture gradients. Because the microwave power absorbed would be proportional to moisture content (ie., water volume) in any small region, and because vapour pressure gradient is proportional to power density (equation 3.3.8), the fields may be expected to produce such a dependence over the entire diffusion-controlled drying phase.

Considering the third of the rate curves of Figure 4.2.1 briefly, two major differences are apparent: a long, very uniform constant-rate phase occurred, and the second critical point appeared much earlier than in either of the other tests. The local peaks in these curves, thought to be microwave resonance effects, are discussed in Section 4.5. Water was added in this test to two 400 ml. beakers set under the centre of the 0.81 $ft.^2$ pyrex tray. Although not measured in detail, the power division between tray and auxiliary load was not as symmetrical as for the two trays (Figure 4.1.3): the auxiliary load absorbed-power increase was minor with volume changes until the wet sand entered the period of rapid total power decrease (below v_w = 600 ml.). Evidently, the rather small change in power input to the bed as moisture decreased was balanced by an increase in drying rate from the hot air; the latter increase was a consequence of the reduced surface temperatures accompanying lower microwave power input. Because the contribution to drying rate of each heat source was approximately the same, such a balancing action is not unreasonable. Emphasis should be placed on the fact that this truly

constant-rate period will not be typical of microwave drying since dielectric losses are usually dependent on moisture content. Only a fully loaded resonant drier should exhibit a constant rate period. Finally, the early demise of the capillary-flow limited phase can probably be attributed to input power decrease rather than to any change in mechanism of moisture movement.

In summary, the fairly detailed examination of this comparatively simple drying situation has brought forth the following points:

i) No constant-rate period will in general be present in microwave drying. The initial period could better be described as an 'external surface evaporation' phase.

ii) To obtain shortest possible drying times, care must be taken to ensure that drying rate is nearly constant as bed saturation moisture content is approached. The external surface evaporation phase will be prolonged by this procedure.

iii) Drying rate during the first falling-rate phase for a porous bed will decrease only slightly with decreasing external evaporating surface. The positive temperature gradient will often keep internal vapour pressures high enough to promote very rapid vapour flow through the bed. A more likely rate-limiting factor is the decrease in power dissipation due to the decreasing amount of lossy material present.

iv) The diffusional drying period should exhibit a linear $\dot{W}$ vs. W characteristic as a result of the tendency of the fields to produce similar vapour pressure gradient and moisture content distributions.

v) Drying should be carried out with low temperature dry air during the capillary-flow limited phase to obtain highest drying rates.

4.3 Dehydration of a Hydrated Inorganic Salt

To further examine the effects of microwave power during diffusion-limited drying, two 1 lb. samples of $CuSO_4 \cdot 5H_2O$ were reduced to the monohydrate form as shown in Figure 4.3.1. Hot air was used in both tests. A more or less constant reduced power was maintained in the second run by the addition of water to a second tray in the cavity. Based on volumes of material in each tray, the power division should have put about 25 to 30% of the total power into the hydrate bed. Because water in a hydrate crystal is tightly bound, the hydrate will be of much lower dielectric loss than an equivalent volume of water. This fact coupled with the relatively small amount of hydrate present (about 375 ml. initially) should have resulted in the power input to the cavity being much less than the $\bar{P}_{d1}$ = 695 watts and $\bar{P}_{d2}$ = 185 watts expected for equivalent water volumes.

In any case, the curves are typical of diffusion-controlled drying. The drying curve for the higher power has two distinct periods for which ln W is proportional to time, a feature of drying where diffusion has controlled for a long period of time. Existence of two periods indicates that a chemical or physical change occurs at some point in the drying. Materials with multimolecular layers of adsorbed water often exhibit similar behavior: the initial phase covers removal of all but the last layer; the final phase involves removal of the much more tightly bound last layer [10].

Before considering the rate curves in detail, an explanation should be made as to why the drying proceeded only so far as the monohydrate form. This arises from the property, peculiar to a mixture of two hydrates of a substance, that the equilibrium constant $\tilde{K}$ is given simply

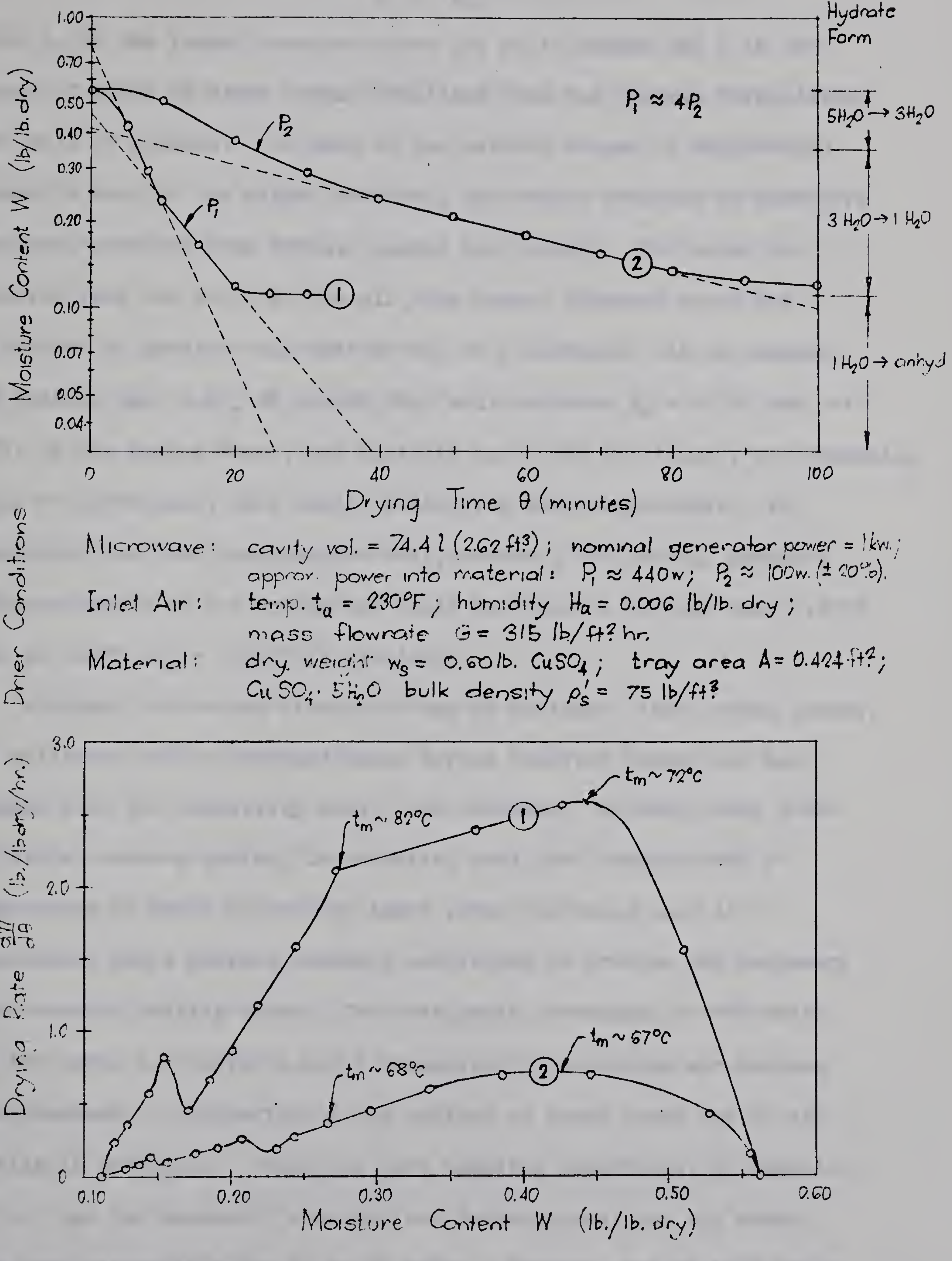

Drier Conditions

Microwave: cavity vol. = 74.4 l (2.62 ft³); nominal generator power = 1kw.; approx. power into material: $P_1 \approx 440$w; $P_2 \approx 100$w. (± 20%).

Inlet Air: temp. $t_a = 230°F$; humidity $H_a = 0.006$ lb/lb. dry; mass flowrate $G = 315$ lb/ft² hr.

Material: dry weight $W_s = 0.60$ lb. $CuSO_4$; tray area $A = 0.424$ ft²; $CuSO_4 \cdot 5H_2O$ bulk density $\rho_s' = 75$ lb/ft³

Figure 4.3.1. Dehydration of $CuSO_4 \cdot 5H_2O$ in a Microwave Tray Drier at 2450 MHz.

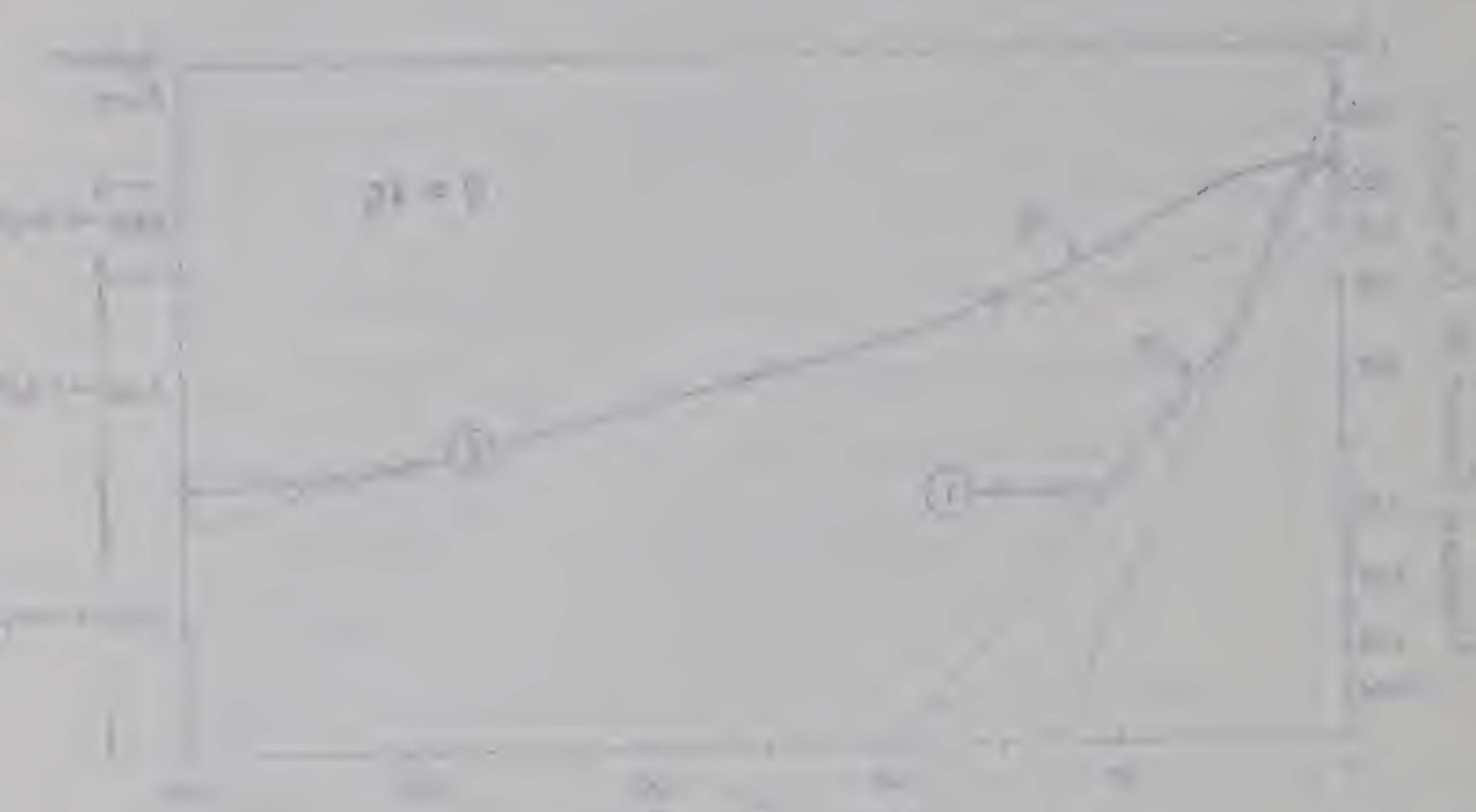

[illegible]

[illegible]

by [14]:

$$\tilde{K} = p_w^{\bar{x}}$$

where p_w is the vapour pressure above the solid phases and $\bar{x}$ is the number of moles of water vapour resulting from the hydrate dissociation (per mole of hydrate). In each of the several stages of dehydration common to most of the higher hydrates, the vapour pressure is therefore constant, provided both hydrate phases are present. For water to transfer from the solid to the air, the vapour pressure above the solid must be greater than that of air at a distance. As an example, the hydrate pair $CuSO_4 \cdot 3H_2O$-$CuSO_4 \cdot H_2O$ will maintain $p_w = 0.135$ atm. at 67°C; in the drying tests, air humidity was 0.006 lb./lb.dry, corresponding to $p_w = 0.0096$ atm., thus easily satisfying this requirement. To accomplish the final dehydration step, however, the partial pressure of water vapour in the drying air would have had to be less than 0.0092 atm. at 100°C ($H_a = 0.0057$ lb./lb.dry).

Although the second rate-curve has no distinct first drying period, its existence will be assumed since drying behavior should not have changed with the relatively small rate increase. In each case, after an initial warm-up period, the material must have reached both a temperature at which all of the input power was being used in evaporation and a surface humidity sufficient to provide the necessary mass transfer driving force. The rate peaks correspond to 465 watts and 125 watts for curves 1 and 2 respectively (including air heating contributions). Estimation of the portion of power input due to air heating is difficult. Using the heat transfer coefficient of equation (4.1.2) and the measured (average) bed temperatures, the air should have been responsible for 45 to 50 watts. However, use of this value of h_c (8.64 BTU/ft.^{2}hr.°F) in a later calculation indicates that h_c

was actually about half of this, so that about 25 watts in each case will probably be closer to fact. Microwave inputs were therefore roughly 440 and 100 watts.

The distinct rate-curve linear segments are likely a consequence of the dehydration $CuSO_4 \cdot 5H_2O \rightarrow CuSO_4 \cdot H_2O$ being a two-stage process; the initial stage $CuSO_4 \cdot 5H_2O \rightarrow CuSO_4 \cdot 3H_2O$ should control drying until negligible pentahydrate remains in the bed. Drying would subsequently be controlled by the slightly more endothermic $CuSO_4 \cdot 3H_2O \rightarrow CuSO_4 \cdot 1H_2O$ decomposition reaction. Occurrence of the breakpoint between the two periods at about W = 0.27 lb./lb.dry rather than at the trihydrate point of W = 0.36 lb./lb.dry is probably due to the high drying rates. When H_s is fairly low and at a sufficiently elevated surface temperature, the monohydrate can exist in a layer near the bed surface. Drying will proceed in this situation with the pentahydrate level moving deeper into the bed (or crystal) at more or less the same rate as the trihydrate level moves. A drying curve typical of the tri- to mono- decomposition should result over the entire dehydration since the kinetics of this reaction will limit moisture movement near the bed surface. As drying rate is increased, H_s will increase to the point at which the monohydrate can no longer exist ($H_s = 0.190$ at $t = 82°C$). Dehydration will proceed according to penta-/tri-hydrate dynamic equilibrium conditions until the rate is again below the critical value. Using equation 3.2.6, the expected drying rate at $H_s = 0.190$ can be calculated:

$$\mathring{W} = \frac{\mathring{w}}{0.6 \text{ lb./lb.dry}} = \frac{h_c A}{0.6 c_s} \left[\frac{-\ln(1 - p_w)}{p_w} \right] \Delta H$$

Inserting values, one obtains:

$$\mathring{W} = \frac{8.64\ (0.424)}{0.6\ (0.33)} \left[\frac{-\ln\ (0.766)}{0.234}\right] (0.190 - 0.006)$$

$$= 3.80 \text{ lb./lb.dry-hr.}$$

This is much higher than the 2.10 lb./lb.dry-hr. observed, likely a consequence of the actual mass transfer coefficient K' being far less than that measured for a free water surface. Decreasing K' by 50%, as was done with h_c in power estimates, leads to much closer agreement with the actual $\mathring{W}$.

The energy of dehydration for the tri- to monohydrate reaction can be calculated from standard heats of formation [25] to be 27.7 kcal./mole. Using an Arrhenius equation to define an activation energy for diffusivity (ie., $\tilde{D} = \tilde{D}_o \exp\{-\Delta H^0/RT\}$) and the slopes for curves 1 and 2 below W = 0.27 lb./lb.dry, an activation energy of 32.8 kcal./gm.-mole is obtained. This would suggest that the temperature of the surface layer for curve 1 was somewhat higher than 82°C; a temperature of 86°C would be sufficient to eliminate the discrepancy.

The effectiveness of microwave energy in this application stems from its ability to produce a large positive temperature gradient. Differentiating equation (3.2.14), one obtains:

$$\frac{dT}{dz} = 2\alpha_d\kappa \left[e^{-2\alpha_d z} - e^{-2\alpha_d d}\right]$$

where

$$\kappa = \frac{0.0966\omega\varepsilon''\ E_o^2}{4k_T\ \alpha_d^2\ (1 + \sqrt{\varepsilon'_r})^2} \qquad \text{... (4.3.1)}$$

Since a vapour pressure gradient has been taken as the diffusional driving force, dp_w/dz must be related to dT/dz. For this, a Clausius-Clapeyron equation is employed:

$$\frac{d}{dT}\left[\ln(p_w/p_o)\right] = \frac{\Delta H^0}{\bar{x}RT^2} \qquad \text{... (4.3.2)}$$

where ΔH^0 = heat of dehydration (cal./gm.-mole)

$\bar{x}$ = number of moles of water vapour released per mole of hydrate

T = absolute temperature (°K)

R = universal gas constant (cal./gm.-mole-°K)

Considering p_w a function of T only, which is in turn a function of z alone, combining the preceding relations gives:

$$\frac{dp_w}{dz} = \frac{dp_w}{dT}\cdot\frac{dT}{dz} = \frac{p_w}{p_o}\left[\frac{\Delta H^0}{\bar{x}RT^2}\right] 2\alpha_d\kappa\left[e^{-2\alpha_d z} - e^{-2\alpha_d d}\right] \quad \ldots (4.3.3)$$

The drying rate of the entire body of material will be determined by the rate of moisture movement across the bed (crystal) surface at z = 0. Evaluating equation (4.3.3) at z = 0:

$$\left.\frac{dp_w}{dz}\right|_{z=0} = 2\alpha_d\kappa\left[1 - e^{-2\alpha_d d}\right]\left[\frac{\Delta H^0}{\bar{x}RT_s^2}\right]\exp\left\{-\frac{\Delta H^0}{\bar{x}RT_s}\right\} \quad \ldots (4.3.4)$$

where T_s = surface absolute temperature (°K).

Under the preceding definition of the parameter κ, the microwave power dissipated in the bed is given approximately by:

$$\bar{P}_d = 4k_T\,\alpha_d^2\,\kappa\left[1 - e^{-2\alpha_d d}\right] \quad \ldots (4.3.5)$$

This allows equation (4.3.4) to be expressed in terms of $\bar{P}_d$ (adjusted for air heating contributions):

$$\left.\frac{dp_w}{dz}\right|_{z=0} = \left[\frac{\bar{P}_d}{2k_T\alpha_d}\right]\left[\frac{\Delta H^0}{\bar{x}RT_s^2}\right]\exp\left\{-\frac{\Delta H^0}{\bar{x}RT_s}\right\} \quad \ldots (4.3.6)$$

Dissipated power has been previously estimated for curves 1 and 2 from observed drying rates at the curve peaks. Using the measured mean bed temperatures as T_s, the ratio of observed drying rates should be obtainable from equation (4.3.6):

$$\left(\frac{\dot{W}_1}{\dot{W}_2}\right)_{calc} = \left(\frac{\bar{P}_{d1}}{\bar{P}_{d2}}\right)\left(\frac{T_{s2}}{T_{s1}}\right)^2 \exp\left\{-\frac{\Delta H^0}{\bar{x}R}\left(\frac{1}{T_{s1}}-\frac{1}{T_{s2}}\right)\right\}$$

$$= \left(\frac{440}{100}\right)\left(\frac{340}{345}\right)^2 \exp\left\{-\frac{27{,}700}{2(1.99)}\left(\frac{1}{345}-\frac{1}{340}\right)\right\}$$

$$= 2.83$$

The observed ratio was 3.60, indicating that the estimated input power ratio is not particularly accurate. Errors in temperature measurement would have only a small effect on the ratio.

Two points are apparent in connection with the drying of hygroscopic materials in microwave fields. The use of microwave power can be expected to result in a very substantial decrease in drying time: a factor of five decrease in drying time was obtained by a factor of four increase in power input. Secondly, the importance of designing a system to provide a positive temperature gradient in the material has been demonstrated. This may require the air flow to be relatively cool if the drying rate is low. Maximum drying rate will be obtained for the highest possible positive internal temperature gradient.

4.4 Discussion of Rate Anomalies

To complete examination of the microwave cavity drying results, a brief attempt to explain the rate curve anomalies will be made. Examples of this behavior can be found in Figure 4.2.1, curve 2, and in Figure 4.3.1, curve 1. In each case, the sudden rate peaking is not readily attributable to changes in drying mechanism, to experimental procedure, or to interpretation of the drying data. An explanation that appears to be compatible with both the drying curves and the experimental conditions is a change in the number of active modes in the cavity with varying moisture content of the material.

An approximate equivalent circuit for the input impedance of a loop-coupled rectangular cavity is given in Figure 4.4.1. The input impedance in terms of the lumped-parameter elements is [2]:

$$Z_{in} = j\omega L_o + j \sum_{k=1}^{\infty} \frac{\omega^3 \tilde{M}_k^2}{L_k(\omega_k^2 - \omega^2 + j\omega\omega_k/Q_k)} \quad \ldots (4.1.1)$$

where: $Q_k = \omega_k L_k/R_k$ = unloaded Q of the kth mode

L_o = self-inductance of the coupling loop

$\tilde{M}_k$ = mutual inductance between coupling loop and kth mode

and $\omega_k^2 L_k C_k = 1$ is the series resonant condition for the kth mode.

For maximum power transfer from the loop to the kth mode, the impedance for this mode must be real (neglecting the effect of L_o, usually a few micro-microhenries for a 1" dia. x 3/8" wide loop). This requirement will be satisfied for $\omega = \omega_k$ at which

$$\left(Z_{in}\right)_k = \omega_k^2 \left(\frac{\tilde{M}_k^2}{R_k}\right)$$

for the kth mode. Because the condition for maximum power transfer coincides with that for mode resonance in the cavity, it follows that the more modes that are present, the more power that the load will absorb. Each mode contribution will of course be different depending upon coupling efficiency and the quality factor Q for the particular mode, but it should be possible to correlate dissipated power magnitude with the number of strongly coupled modes in resonance. If the drying rate curve anomalies are due to such power peaking, they should occur at dielectric conditions under which the number of modes has reached a local maximum.

For relative simplicity, a sand drying curve (Figure 4.2.1, curve 2)

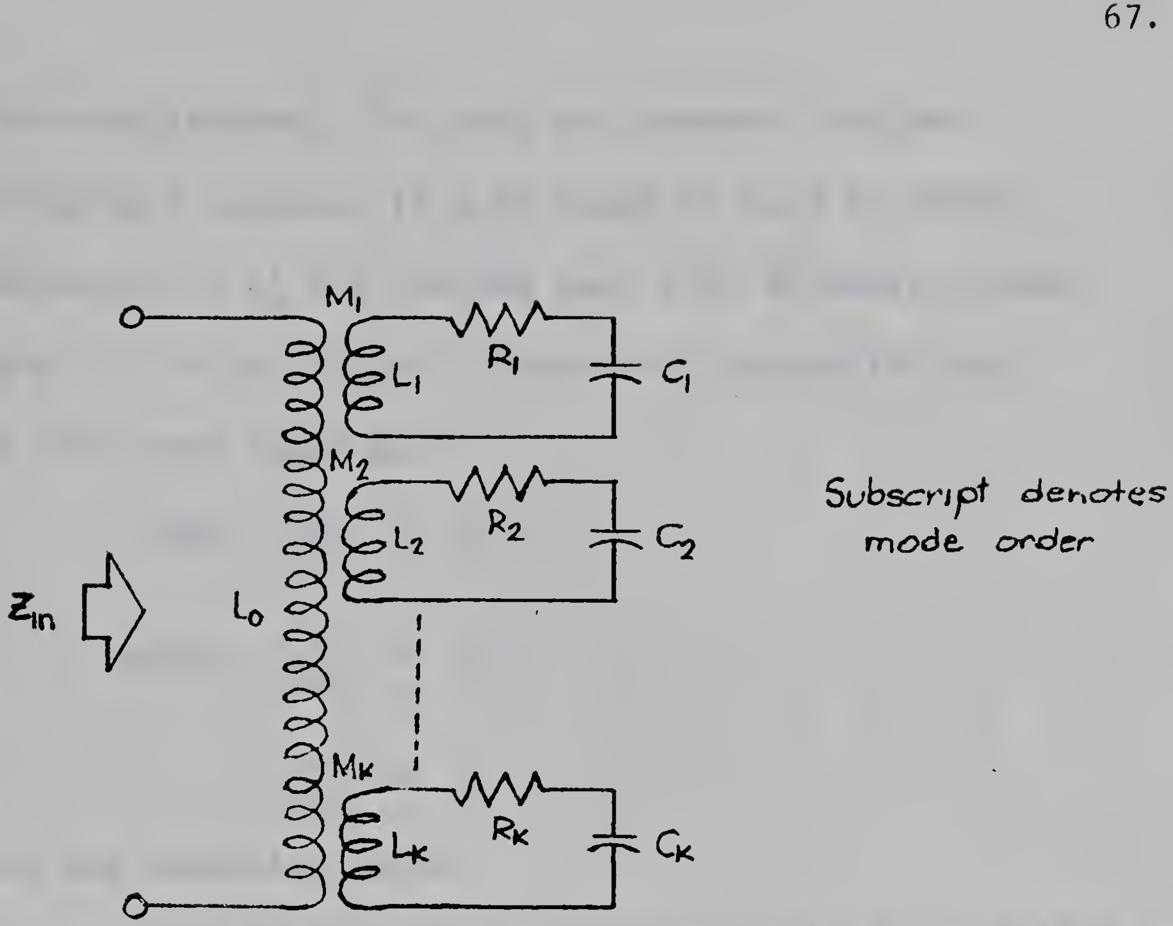
M1
R1
L1
C1
M2
R2
L2
C2
Subscript denotes mode order
Zin
L0
Mk
Rk
Lk
Ck

Figure 4.4.1. Lumped-parameter Equivalent Circuit of a Loop-coupled Multi-mode Cavity

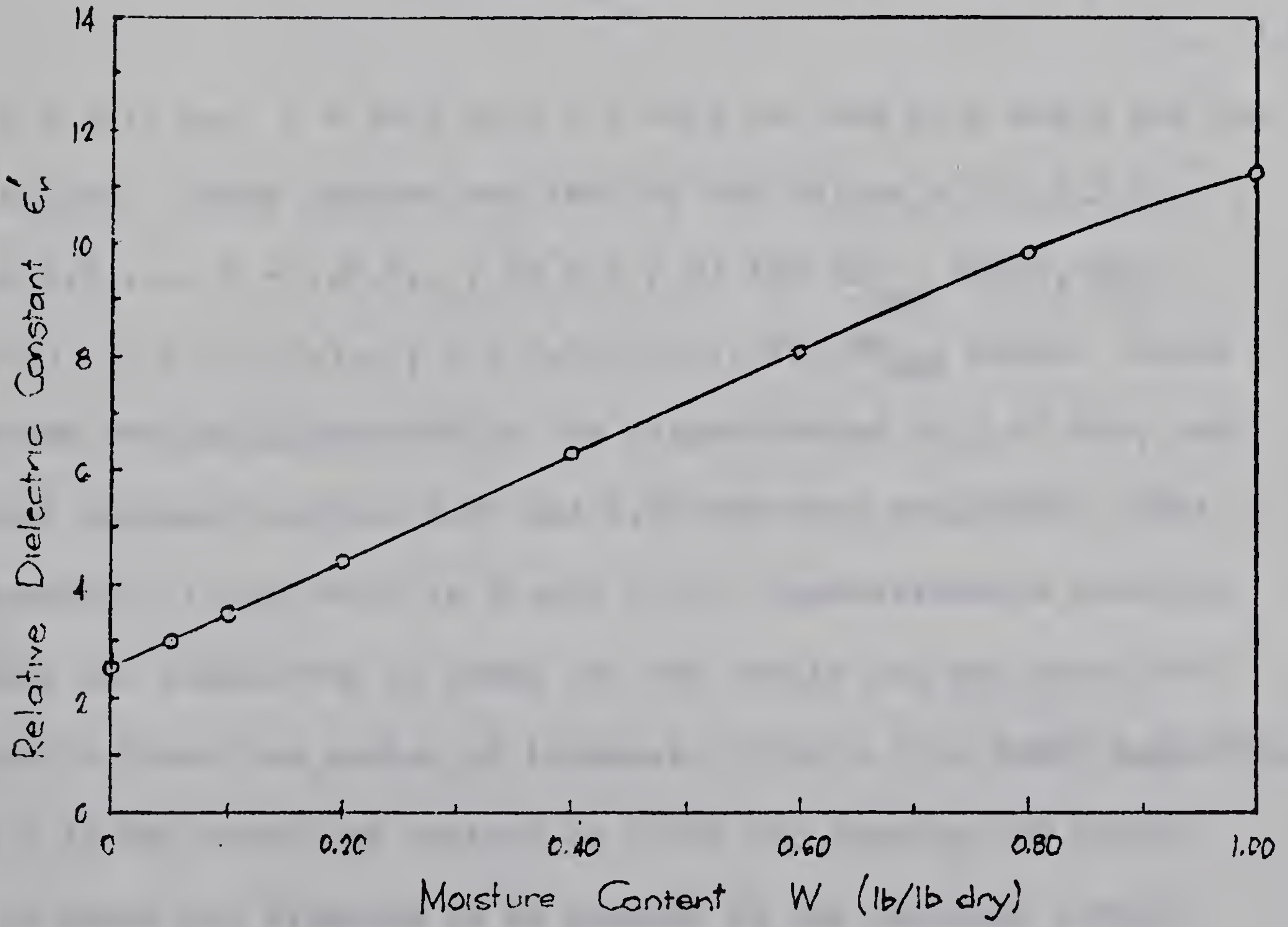

Figure 4.4.2. Calculated Dielectric Constant Variation of a Wet Sand with Moisture Content

was chosen for the calculations. The sand was assumed lossless compared to water so that equation (3.1.5) could be used to obtain an approximate variation of ε_r' for the wet sand with moisture content between W = 0 and W = 1.00 lb./lb.dry. Dielectric values for the sand and water at 50°C were taken as:

$$\text{sand:} \quad \varepsilon_{sr}' = 2.50$$

$$\text{water:} \quad \varepsilon_{wr}' = 70$$

$$\varepsilon_{wr}'' = 7$$

Figure 4.4.2 shows the resulting curve.

The resonances possible in an unloaded 38.5 cm. x 40.0 cm. x 48.5 cm. cavity were next calculated using

$$(f_r)_{mnp} = \frac{1}{2\sqrt{\varepsilon_o \mu_o}} \left[\left(\frac{m}{a}\right)^2 + \left(\frac{n}{b}\right)^2 + \left(\frac{p}{c}\right)^2 \right]^{1/2} \qquad \ldots (4.4.2)$$

where a = 38.5 cm., b = 40.0 cm., c = 48.5 cm. and m, n and p are the mode indices. These indices may take on the values m = 0,1,2,3,..., n = 0,1,2,3,..., p = 1,2,3,.., (m = n ≠ 0) for TE_{mnp} modes, and m = 1,2,3,.., n = 1,2,3,.., p = 0,1,2,3,.., for TM_{mnp} modes. Since the system was being operated in the neighbourhood of 2.45 GHz, only the modes resonant between 2.20 and 2.60 GHz were evaluated. This mode spectrum, illustrated in Figure 4.4.3, demonstrates a relative abundance and regularity of modes for the cavity and was more than adequate to cover the region of interest. With a 1 kw DX260 magnetron having a 15 MHz bandwidth centred on 2.460 GHz feeding the cavity, about 20 modes are expected to be present in the unloaded system.

To take into account the effect of dielectric loading on the cavity, the tray with wet material was considered to fill the entire

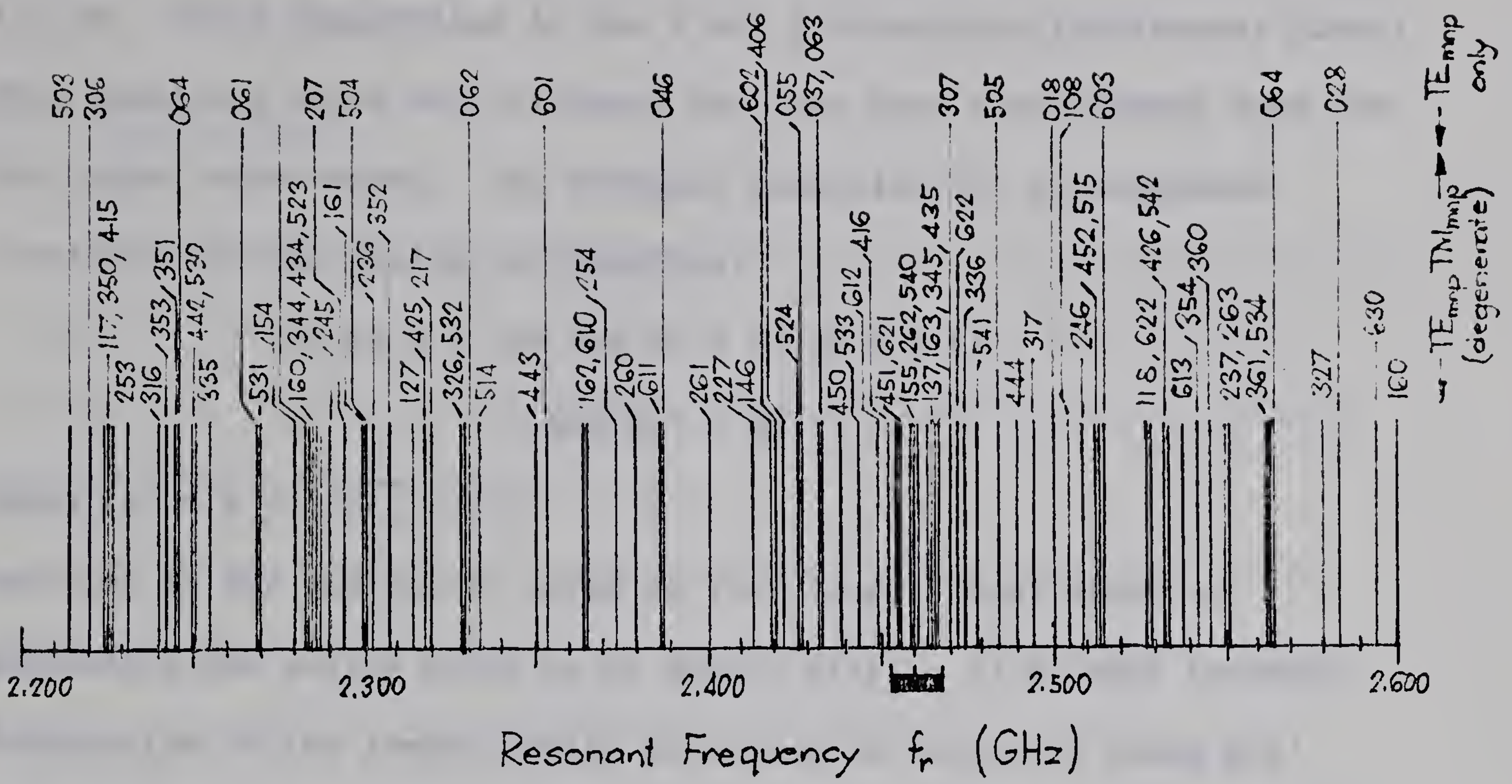

Figure 4.4.3. Resonant Frequency Spectrum of the Unloaded 38.5 x 40.0 x 48.5 cm Cavity near 2.46 GHz

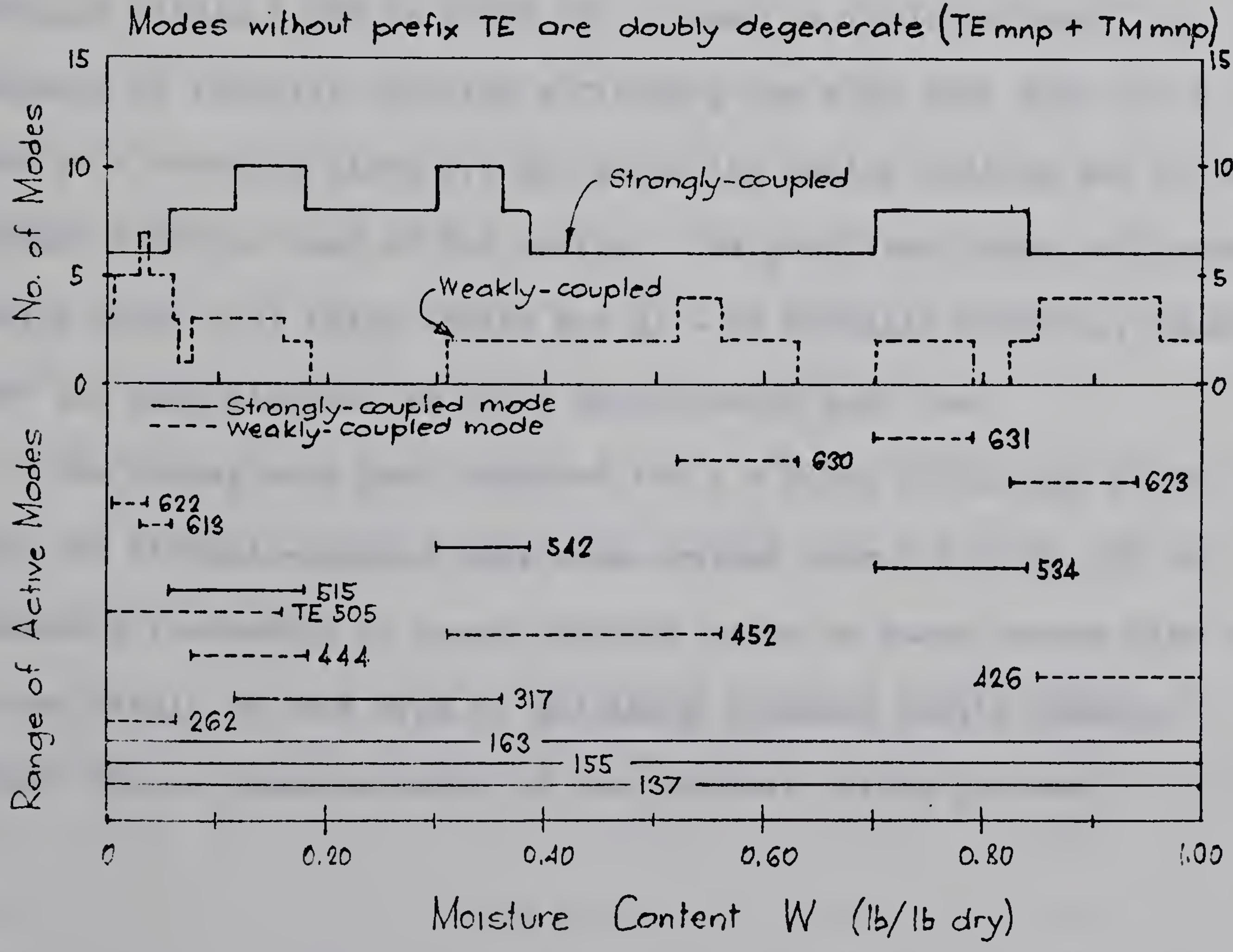

Figure 4.4.4 Resonant Modes in the Loaded Cavity for Drying of a 1.5 cm deep Sand Bed

horizontal cross-section at a uniform and constant thickness of 1.5 cm. Field distortions in the x and y directions (horizontal plane) were neglected since bed thickness was less than a wavelength even for the higher order modes. The resonant condition for z-components (vertical) of the fields is therefore:

$$\sin kz = 0 \quad \text{or} \quad \cos kz = 0 \quad \text{at } z = a'$$

$$\text{and } ka' = m\pi$$

where $a' = a + d(\sqrt{\epsilon_r'} - 1)$

Addition of the dielectric layer is very roughly equivalent to separating the cavity walls by an amount $d(\sqrt{\epsilon_r'} - 1)$ so that resonant frequencies of the loaded cavity modes can be estimated using m/a' in place of m/a in equation (4.1.2). When this is done, the mode chart of Figure 4.4.4 is obtained: the line segments indicate the moisture content range in which each particular mode should be resonant within 2.452 to 2.468 GHz. Based on field patterns, an estimate of relative coupling efficiency has also been made for a loop in a vertical plane 6.5 cm. below the cavity ceiling and 9.0 cm. forward from the rear of the cavity. The predicted number of loaded cavity modes (33) falls within the 31 - 37 actually measured, indicating that the approximation is not a particularly poor one.

The drying rate peak observed for W = 0.180 lb./lb.dry falls into the strongly-coupled mode peak centred over W = 0.16. It is therefore reasonable to expect similar peaks on other curves also to be the result of this type of multimode resonant cavity behavior rather than a characteristic of the physical drying process.

5.0 AN ECONOMIC EVALUATION OF MICROWAVE DRYING

5.1 Capital Costs

The economics of a microwave drying system will be discussed from a general standpoint in the following sections. For more specific information, current papers dealing primarily with microwave heating economics should be consulted [5,6].

A microwave drier will usually consist of the generator and its power supply, a drying enclosure, an air system, a material conveying system, and suitable instrumentation and controls. Units in which microwave energy is used to dry only in low moisture content regions will include a heater in the air system. By comparison with conventional hot air drier components, it is apparent that microwave drier economics will suffer from the additional first cost of both the generator and power supply and possibly some enclosure or applicator modifications which may be necessary to properly carry and confine the microwave fields. This will be offset to a varying extent in other types of driers in which, for example, microwave heating energy replaces a steam system. In any case, to allow a comparison with conventional driers, it will be necessary to know an approximate cost of the microwave system; costs for other components should be similar to those for standard driers of the same physical size.

Disman [5] has provided figures on tube and power supply costs which should serve for a conservative current estimate. Costs range from $175/kw for 25 kw DC power supplies to $125/kw for 500 kw DC power supplies. Tube costs in small quantity lots vary from about $80/kw at 100 kw output to $120/kw for 1 kw units. These figures apply mainly to

the magnetron type generator. Ordered in large quantities, a normal manufacturing cost decrease should lower unit prices by 30 to 40%. To these basic costs must be added allowances for tube and installation hardware, installation labour, and any equipment necessary for control and safety systems. In most applications, such costs may range from 100% to 175% of the basic device totals. A complete microwave generator for 25 kw output should therefore cost in the neighbourhood of $600 to $800 per kw.

The prices of drier additions for microwave application are more difficult to establish. In some instances, the drier can be designed as an inherent applicator for which limited additional costs should be expected; a multimode cavity used as a cabinet or tunnel drier is an example. A slotted waveguide applicator installed in a drying tunnel on the other hand will obviously increase the microwave tunnel price by at least the manufacturing and installation cost of the applicator system. It should be noted that use of microwave energy will substantially reduce the selection of materials which can be allowed within the applicator. Trays, belting, conveyor idlers, supports, air ducts and similar items likely to be located in the fields must be made of very low dielectric loss materials such as polypropylene and teflon. Necessary metallic parts must be designed into the applicator as part of the guiding structure if such difficulties as arcing are to be avoided. Both the additional care required in design and the restricted material selection can be expected to increase costs beyond those of an equivalent physical size conventional drier.

Emphasis should be placed on the point that the cost disadvantages noted apply to a microwave drier of configuration and dimensions

similar to a standard drier counterpart. Because use of microwave energy will generally increase drying rates, the microwave drier will have a definite advantage in product capacity. Alternately, for a given product capacity, a microwave drier should be considerably smaller than an equivalent capacity conventional unit. Much of the apparent capital cost disadvantage of a microwave system may be offset by this feature alone.

5.2 Operating Costs

Until very recently, high power at microwave frequencies was available only at relatively high cost. It is quite common to find notes of 'very expensive' and 'power costs may range to ten times conventional fuel costs' in drier design reference sections describing dielectric drying. While such statements covered conditions existing into the early 1960's, they are now extremely pessimistic and will probably serve to slow the acceptance of this technique in many industries.

Operating costs are properly divided into four main categories:

1. Direct fuel, power, maintenance and replacement costs
2. Drier amortization costs
3. Labour costs
4. Indirect costs which arise from the drier being part of a plant. Included here would be such costs as lighting, floor space, administrative overhead and taxes.

Since equipment capital cost directly affects overall operating cost, drier economic evaluation can be quite reasonably based on a comparison of operating costs alone. Drier operating costs however, are commonly stated in terms of 'cents-per-pound of water evaporated'

based only on labour, power, fuel and maintenance costs. To allow comparison with such figures, the following discussion will establish an equivalent microwave drier operating cost rather than the complete cost described.

The highest single cost in the operation of a microwave power system is, and will remain so for several years, the cost of tube replacement. Tube life presently ranges between 2500 and 10,000 hours so that a figure of 3000 hours can be used as a conservative basis for replacement cost estimates. A tube cost of about 1.2¢ per lb. of water evaporated results for an applicator efficiency of 80 percent. Power supply maintenance can usually be neglected in comparison with the tube replacement costs.

Power costs for a microwave drier can be calculated on the basis of 55 percent conversion efficiency for klystron tubes, 75 percent for magnetrons and 95 percent for power supplies. A 1¢/kw-hr. prime power rate would therefore present a microwave energy cost of from 0.5 to 0.7¢/lb. of water evaporated, depending upon whether klystron or magnetron generators were used. Because air heating costs are usually well below this in conventional driers, fuel costs can be neglected in driers in which microwave energy is the primary drying heat source. If microwave power is used as an auxiliary system, the above costs should be added to conventional system fuel and power costs.

Because microwave driers will probably require some power control equipment to make most efficient use of input power, they will consequently tend to be more highly automated overall than conventional driers. In many systems, this should result in a decreased number of operating personnel per drier being required so that a labour cost reduction should be expected. The automatic control philosophy will

also fit more readily into continuous processing or computer-controlled applications. In any case, labour costs will have to be worked out for each particular application since they strongly depend on device type, process requirements and plant operating procedures.

Although these figures do not nearly constitute complete drier costs, they will establish in conjunction with readily available conventional drier cost data approximate costs for similar microwave equipment. Until microwave driers come into more common usage, reliable cost data will be scarce and evaluation will have to be based on such extensions to known drying applications.

5.3 Comparison with a Conventional Drier

To illustrate the preceding comments, a simple drying application will be evaluated briefly from both conventional and microwave drier standpoints. The batch drying of finely powdered, heat-sensitive materials such as dyes or blood fractions can be used as an example. Because of the heat sensitivity, air temperatures of less than 180°F must be used. As the material begins to dry at the bed surface, air velocities must also be kept low to prevent excessive material entrainment losses. Both requirements will tend to make a conventional cabinet-and-tray drier quite inefficient.

A microwave drier, however, offers several advantages. If bed temperature is used to control power input, drying can be made to proceed at an optimum rate for a fixed bed by maintaining the 180°F maximum allowable temperature. If the drying air is kept at about 120°F and dessicated if necessary to provide sufficient moisture handling capacity, a reasonably large vapour pressure gradient will exist and drying should proceed quite rapidly. Since drying rate

usually increases much faster than bed temperature, a more favourable time-temperature situation is possible using the higher drying rates of microwave power. The chances of product spoilage are reduced as a result. Providing the material is mechanically de-watered before loading into the drier, no auxiliary air heating system should be necessary for the microwave drier; a capital cost item can therefore be deleted.

Based on the copper sulphate hydrate drying results, it is not unreasonable to anticipate a microwave drying time some 90% less than the air drying time for a fairly non-porous material. A much smaller drier should be possible for a microwave system with consequent savings in cabinet cost, floor space requirements, and blower cost.

Typical figures for a medium size tray drier are presented in Tables 1, 2 and 3. Sizing is relatively conservative as are the costs. The purpose of this evaluation is not to demonstrate cost advantages using microwave power but to illustrate the various cost factors involved, their relative magnitudes, and the effect of product quality, losses, and handling costs on the overall economics. The areas of respective advantage are apparent; also apparent is the tremendous effect of tube replacement costs on the microwave drier economics. A good case for maximum effort to increase tube life certainly exists. Similarly, both tube and power supply initial cost reductions would greatly enhance the microwave economics.

The following notes are added to supply some terms of reference for the drier evaluations which were not included in the body of Tables 2 and 3:

(1) Drying times include an allowance for loading and removal of trucks.

Table 1. Drier Evaluation: Typical Product Specifications and Drier Schematic Diagrams

PRODUCT SPECIFICATIONS
Heat-sensitive, non-porous powder
Value: $1.00/lb.
Moisture content: Initial = 0.30 lb./lb.dry; Final = 0.01 lb./lb.dry
Max. allowable material temp.: 180°F
Max. allowable air velocity: 225 fpm

TRAY DRIER SCHEMATIC DIAGRAMS

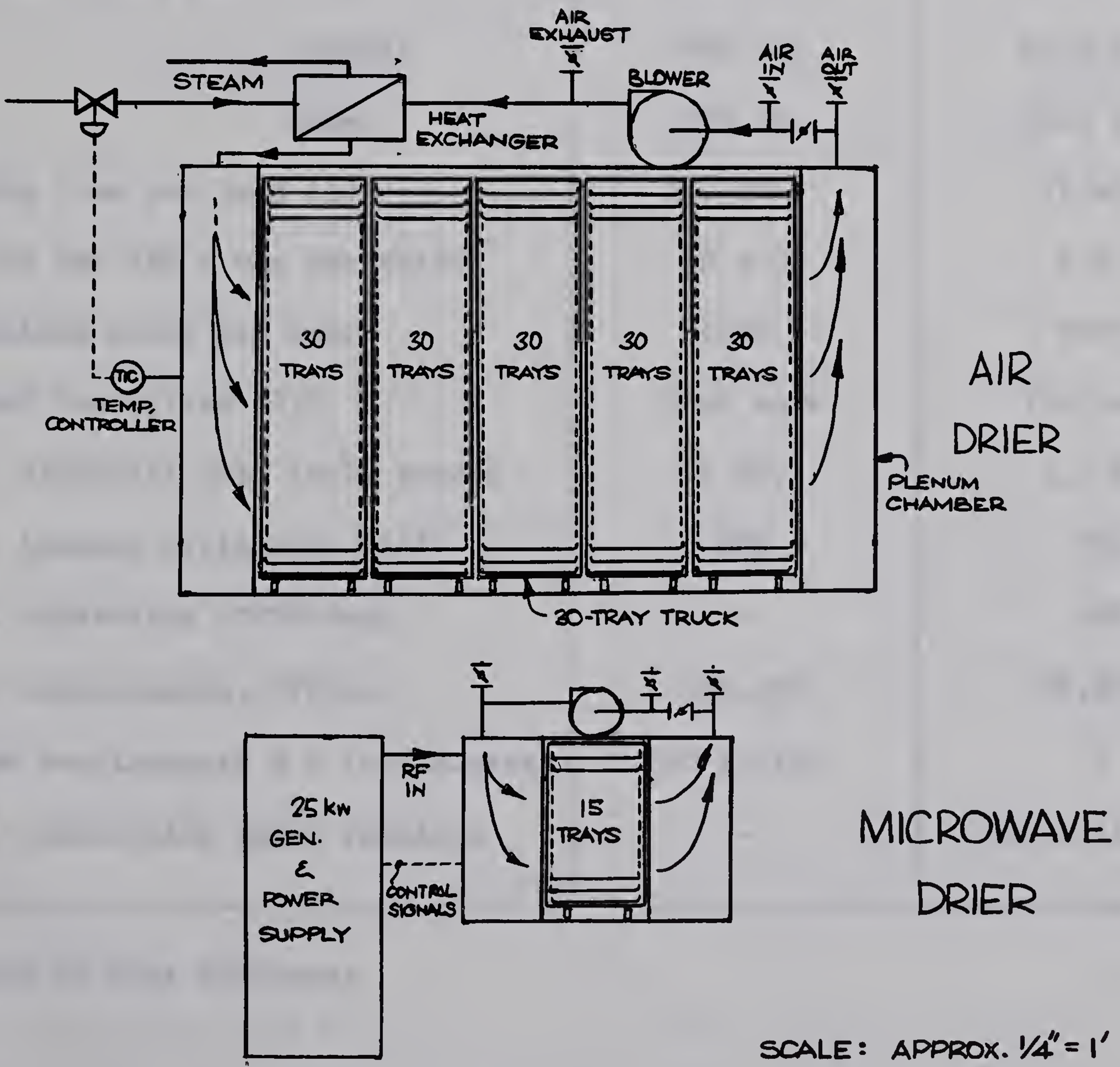
AIR EXHAUST
STEAM
BLOWER
AIR IN
AIR OUT
HEAT EXCHANGER
30 TRAYS
30 TRAYS
30 TRAYS
30 TRAYS
30 TRAYS
TIC
TEMP. CONTROLLER
AIR DRIER
PLENUM CHAMBER
30-TRAY TRUCK
RF IN
25 kw GEN. & POWER SUPPLY
15 TRAYS
CONTROL SIGNALS
MICROWAVE DRIER

SCALE: APPROX. 1/4" = 1'

BOTH DRIERS RATED 50 lb.water/hr.

Table 2. Drier Evaluation: Specifications for Air and Microwave Tray Driers Suitable for Moderately Heat-Sensitive Powders

DRIER SPECIFICATIONS	AIR	MICROWAVE
Evaporative capacity	50 lb./hr.	50 lb./hr.
Cabinet dimensions	13.0' x 3.5' x 8'	5' x 3.5' x 3.5'
Floor space required (5)*	36' x 16'	17' x 16'
Total no. of trays x spacing	150 x 3"	15 x 2.5"
No. of tiers x trays per tier	5 x 30	1 x 15
Tray dimensions	24" x 36" x 1"	24" x 36" x 1"
Tray loading	1 lb./ft.^{2}	1 lb./ft.^{2}
Initial drier load: wet	900 lb.	90 lb.
product	692 lb.	69.2 lb.
water	208 lb.	20.8 lb.
Drying time per load (1)*	250 min.	25 min.
Shifts per day x men per shift	2 x 2	2 x 2
Operating hours per year	5000	5000
Blower capacities (2)*	2500 scfm	750 scfm
Aux. electical load incl. motors	4 HP.	1.5 HP.
Avg. thermal efficiency (3)*	30%	80%
R.F. conversion efficiency	-	60%
Heat requirements, BTU/hr.	183,300	68,800
Steam requirements @ 4 lb./lb.water	200 lb./hr.	-
R.F. output/line input required	-	20.2 kw/33.6 kw

*Refer to text for notes

Table 3. Drier Evaluation: Capital and Operating Costs

CAPITAL COST (Installed)	AIR		MICROWAVE	
Cabinet	4000		1000	
Trucks and trays	4000		1500	
Building space @ $15/ft.^{2} (5)*	8600		4100	
Air system and blower	1000		500	
Air heater and controls	2000		-	
Instrumentation	1000		1000	
25 kw Microwave gen. and pwr. supply	-		15,000	
Totals	20,600		23,100	
Cost of capital @ 6%/yr./operating life	24,700/20 yrs.		27,800/20 yrs.	
OPERATING COSTS	AIR		MICROWAVE	
	$/yr.	¢/lb.	$/yr.	¢/lb.
Direct:				
Steam @ $1.50 per 1000 lb.	1500	0.600	-	-
Electricity @ 1¢/kw-hr.	150	0.060	1680	0.671
Maintenance @ 3% of cap. cost (6)*	460	0.184	655	0.263
Tube replacement cost (7)*	-	-	4160	1.666
Sub-Total	2110	0.844	6495	2.600
Yearly amortization costs	2260	0.906	2540	1.020
Labour costs @ $7500/man-yr.	30,000	12.000	30,000	12.000
Indirect:				
Allow 25¢/100¢ of labour cost	7,500	3.000	7,500	3.000
Total	41,870	16.750	46,535	18.620
Other Possible Costs				
Fines entrainment loss @ 0.1%	833	0.333	negl.	-
Product spoilage by overheating @ 0.5%	4160	1.667	negl.	-

*Refer to text for notes

(2) Capacity for the air drier is sufficient to provide the required heat input for an exhaust temperature of 120°F; the tray spacing was increased to 3" to stay below the velocity limit of 225 fpm. The microwave drier blower was sized to provide necessary moisture capacity for a humidity difference [$(H_s - H_a)$ x 40%] of 0.025 lb./lb.dry.

(3) Direct batch driers generally use from 2.5 to 8 lbs. of steam per lb. of water evaporated (Perry [17]); the 30% efficiency figure used is considered representative and perhaps slightly optimistic. For the microwave drier, the 80% is applicator efficiency.

(4) Power supply and generator are included in this figure. Because 25 kw units are becoming reasonably common, their slightly more advanced development state should justify the overall efficiency assumed.

(5) For the air drier, 11.5 feet on either end and a 12 foot wide frontage area were allowed for handling and storage of the large number of trays necessary with this drier. In the microwave case, a 4 ft. x 4 ft. area was assigned to the power supply with an additional 4 feet on either end of the drier and a 12 foot wide frontage area allowed for tray handling.

(6) The cost basis for these figures is capital cost less building space costs.

(7) A tube cost of $2500 and an operating life of 3000 hours have been assumed.

5.4 The Potential of Microwave Drying

To date, the main applications of microwave power to drying have involved food products, such as the final drying of potato chips [27], and lumber, in which veneer redrying has received much attention [28]. About 45 ten kilowatt or larger systems are presently in operation in the United States with over half of these in drying applications. However, a large percentage of driers require at least 250,000 BTU/hr. of input heat (or approximately 100 kw of microwave energy input to the drier) and it is in these relatively high power systems that microwave power has so far made the least progress. Several factors have combined to slow its more general acceptance for higher power applications.

Of these factors, the lack of information concerning the effect of microwave energy on materials is perhaps the greatest stumbling block. In the drying of lumber for example, no reliable means exists, besides actual tests, to predict the maximum allowable power density, the rate of moisture transfer, or the long-term effect, if any, of the electromagnetic energy on natural wood preservatives. A similar problem faces applications in the drying of grains, foods, and pharmaceuticals. Many materials also exhibit peculiar dielectric characteristics such as becoming extremely lossy quite suddenly under certain conditions of temperature and composition [24] - behavior which would seriously limit the effectiveness of microwave power if exact details of the cause and conditions were not known. A considerable quantity of useful data has been accumulated for wood products drying, however, and empirical design relations are beginning to appear. This will almost certainly encourage further applications activity in wood products industries where slow, expensive drying processes are often necessary.

A second deterent to wider microwave power usage is the current high cost of generation equipment. The technology of high power, stable, electronic power supplies is being developed along with the generators so that the costs of both should decrease with time at more or less the same rate. With the construction of more equipment involving high power microwave, whether for cooking, drying, or particle acceleration, one or more of the large generator sizes should move into the status of a production item. Costs can be expected to drop sharply below those presented here for such units. Along with this, a tube rebuilding or exchange program would greatly decrease the tube replacement component of operating cost. Disman [5] estimates that a tube can be rebuilt several times for 20% to 40% of the original cost each time. Development of tubes with very long lives would similarly reduce this major cost factor.

As with many new industrial techniques, microwave power suffers from an aura of complexity. Process designers are generally not familiar with microwave systems and so would tend to be quite suspicious of microwave-based equipment. The manufacturers of microwave power hardware and process equipment could do well to focus their advertising effort on education of user personnel and process engineers in order to remove the familiarity, if not the understanding, barrier. Applications should be approached from a process standpoint, however; electronic engineering terminology and terms of reference are usually unintelligible to such groups.

Other problem areas exist, but these are shared in many cases by conventional drying equipment. The obstacles to microwave power acceptance just described are far from insurmountable and in all likelihood will cease to be problems within five years. During this

time, the full potential of microwave power will become apparent as the technique establishes itself. Applications requiring rapid moisture transfer, high thermal efficiency, compact equipment, low drying temperatures, containment within glass, or reduced pressure drying should all find considerable advantage in the use of microwave power for drying.

6.0 CONCLUSION

The benefits of microwave power in the form of increased drying rates, suitability for drying heat-sensitive, hygroscopic or non-porous materials, drier design flexibility, and potential economic advantages have been established on a reasonably sound basis. As might have been expected, no sweeping superiority of the technique is evident. Rather, in common with all other drying methods, microwave drying has a specific range of applicability within which its advantages, both physical and economic, are substantial.

Because of recent advances in the technology of microwave power, its range of applicability to drying is becoming increasingly broad. Microwave drying can therefore be considered a feasible and potentially valuable industrial drying process.

REFERENCES

1. Babbitt, J. D., "Observations on the permeability of hygroscopic materials to water vapour", Can. J. Research, Vol. 18A, pp. 105-121 (NRC No. 907).

2. Collin, R. E., Foundations for Microwave Electronics, McGraw-Hill, 1966, p. 691.

3. Crank, J., The Mathematics of Diffusion, Clarendon Press, Oxford, 1956.

4. Dekker, A. J., Solid State Physics, Prentice Hall, 1957, pp. 133-159.

5. Disman, M., "An Economic Model for Microwave Heating Systems", J. Microwave Power, Vol. 1, 1966, pp. 33-42.

6. Goerz, D. J. and Jolly, J. A., "The Economic Advantages of Microwave Energy in the Paper Industry", 1967 Symposium on Microwave Power, Stanford University, Stanford, California, March 1967.

7. Harrington, R. F., Time-Harmonic Electromagnetic Fields, McGraw-Hill, 1961.

8. Henderson, S. M., "A basic concept of equilibrium moisture", Agr. Eng., Vol. 33, pp. 29-32.

9. James, R., Tinga, W. and Voss, W., "Some Factors Affecting Energy Conversion in a Microwave Cavity", J. Microwave Power, Vol. 1, 1966, p. 97.

10. Jason, A. C., "A study of the evaporation and diffusion processes in the drying of fish muscle", Soc. Chem. Ind., 1958, pp. 103-135.

11. Knowlton, A. E., Standard Handbook for Electrical Engineers, McGraw-Hill, 1957, Ninth Ed., p. 475.

12. Lewin, L. Advanced Theory of Waveguides, Iliffe and Sons, London, 1951, p. 156.

13. McCabe, W. L., and Smith, J. C., Unit Operations in Chemical Engineering, McGraw-Hill, 1956.

14. Maron, S. H., and Prutton, C. F., Principles of Physical Chemistry, MacMillan, 1958, pp. 366-369.

15. Marshall, W. R. Jr., and Hougen, O. A., "Drying of Solids by Through Circulation", Trans Am. Inst. Chem. Eng., Vol. 38, pp. 91-121, 1942.

16. Newitt, D. M., and Corben, R. W., "Mechanism of drying of solids. VI. The drying characteristics of granular porous material", Trans. Inst. Chem. Engrs., Vol. 33, 1955, pp. 52-63.

17. Perry, J. H. (editor) Chemical Engineers Handbook, 4th Ed., McGraw-Hill, 1963.

18. Shepherd, C. B., Brewer, R. C., and Hadlock, C., "Drying materials in trays. Evaporation of surface moisture", Ind. Eng. Chem., Vol. 30, 1938, pp. 388-397.

19. Van Arsdel, W. B., "Approximate diffusion calculations for the falling rate phase of drying", Chem. Eng. Prog., Vol. 43, 1947, pp. 13-24.

20. Van Arsdel, W. B., Food Dehydration, Vol. I, Avi, 1963.

21. von Hippel, A. R., Dielectric Materials and Applications, M.I.T. Tech. Press and John Wiley, 1954.

22. Roberts, K. and von Hippel, A. R., "New Method for Measuring Dielectric Constant and Loss in the Range of Centimeter Waves", J. Appl. Phys., Vol. 17, 1946, p. 610.

23. Voss, W. A. G., "Factors Affecting the Operation of High Power Microwave Heating Systems for Lumber Processing", I.E.E.E. 1GA2, No. 3, 1966, pp. 234-243.

24. Voss, W. A. G., Tinga, W., "A Materials Evaluation Technique for Microwave Power Processing", Symposium Paper E2, The International Microwave Power Institute 1967 Symposium, Stanford, California.

25. Weast, R. C., Handbook of Physics and Chemistry, 45th Ed., 1964, Chemical Rubber Co. Cleveland, Table D-41.

26. Brunauer, S., Emmett, P. H. and Teller, E., "Adsorption of gases in multimolecular layers", J. Am. Chem. Soc., Vol. 60, 1938, pp. 309-319.

27. O'Meara, J. P., "Progress Report on Microwave Drying", Annual Conference of the Potato Chip Institute International, 1966, Las Vegas, Nevada.

28. Gruber, G., "Practical Aspects of Microwave Veneer Redrying", J. Microwave Power, Vol. 2, 1967.

B29868